Effect of Fly Ash and Nanosilica on Concrete Compressive Strength at Early Age

by

Nitza M. García Berrios

A thesis submitted in partial fulfillment of the requirements for the degree of
MASTER OF SCIENCE
in
INDUSTRIAL ENGINEERING
UNIVERSITY OF PUERTO RICO
MAYAGÜEZ CAMPUS
2015

Approved by:

Saylisse Dávila, PhD Member, Graduate Committee	Date
Wandaliz Torres, PhD Member, Graduate Committee	Date
Mauricio Cabrera, PhD Co-President, Graduate Committee	Date
O. Marcelo Suárez, PhD President, Graduate Committee	Date
Rémi Mégret Representative of Graduate Studies	Date
Viviana Cesaní, PhD Department Director	Date

ABSTRACT

The decision making process in modern construction industry is challenging when recycle materials are required. One such approach is the replacement of cement by fly ash. Unfortunately, this replacement lowers concrete's compressive strength at its early age. To counterbalance this loss, nanosilica is being utilized. The relationships among different components upon concrete fabrication require a design of experiments with mixtures to model concrete compressive strength. A single criteria optimization strategy was adopted to recommend mixture combinations that maximize the compressive strength. The results serve as a guide to control the additions of these mineral admixtures to design a material that withstands a desired level of compressive strength. The second stage of this work encompasses the use of a multiple-criteria optimization method to optimize several concrete performance measures simultaneously, namely concrete density, porosity, and compressive strength. This approach allows recommending mixtures that contain the mineral admixtures, in addition of conventional mixtures.

RESUMEN

El proceso de toma de decisiones en la industria de la construcción actual es complejo cuando se requieren materiales reciclables. Un enfoque de este tipo es el reemplazo de cemento por ‘fly ash’. Desafortunadamente, éste reemplazo reduce la resistencia a compresión del concreto durante su edad temprana. Para contrarrestar esta pérdida, sílica nano-estructurada está siendo utilizada. La relación entre diferentes componentes en la fabricación de concreto requiere un diseño experimental con mezclas para modelar la resistencia a compresión del concreto. Una estrategia de optimización de un solo criterio fue adoptada para recomendar combinaciones de mezclas que maximicen la resistencia a compresión. Los resultados sirven como guía para controlar las adiciones de estos aditivos minerales para así diseñar un material que soporte cierto nivel de resistencia a compresión. La segunda etapa de este trabajo incluye el uso de una metodología de optimización multi-criterio para optimizar ciertas medidas de desempeño del concreto simultáneamente, llamadas densidad, porosidad, y resistencia a compresión. Este enfoque permite recomendar mezclas que contienen los aditivos minerales, además de las mezclas convencionales.

To my grandparents, Norma Iris Rivera and Luis García, for being my inspiration and teaching me to have love for my studies.

ACKNOWLEDGMENTS

I would like to give my thanks to my advisor Dr. Oscar Marcelo Suárez and co-advisor Dr. Mauricio Cabrera for their guidance and help during the whole process of this research. Thank you both for sharing your knowledge with me, I appreciate your dedication for research. In addition, I want to thank Dr. Saylisse Dávila and Dr. Wandaliz Torres for their advice and assistance during the execution of this research as members of my committee. Thanks to the Department of Industrial Engineering of the University of Puerto Rico at Mayagüez (UPRM), their professors, and administrative personnel. Also, thanks to the Department of Civil Engineering for the use of the laboratories and to the lab technicians for their help.

This work was supported by the National Science Foundation under Grants No. HRD 0833112 & 1345156 (CREST program). Additional support was provided by the US Department of Education through Grant No. P120A120097 (MSEIP program). I would like to thank to these programs for support me financially through these years.

I am very grateful to Dr. Luis E. Zapata and Hildelix Soto for their advice in the area of Civil Engineering. I want to give my special thanks to my undergraduate students Carlos Medina, Giovanny Torres, Elizabeth de la Cruz, and Marivette Rullán for their help with the mixtures preparation and testing procedures at the laboratory.

I want to give my thanks to the graduate students at UPRM; especially to Katia Iris Camacho, Lesley Rivera, Yaileen Méndez, Samuel Bonet, Esmeralda Niño, and Yaritza Santiago for being my partners and friends during these years. I really have good memories with you guys. My dear Juan Fernando Rosas: thank you. Thank you for all your help and support for this work. Finally, thank you to my family for always being there for me.

TABLE OF CONTENTS

LIST OF FIGURES

LIST OF TABLES

NOMENCLATURE

SCM: supplementary cementing materials

MA: mineral admixture

PC: Portland cement

FA: Fly ash

nS: nanosilica

w/b: water to binder ratio

SF: silica fume

DOE: design of experiments

SP: superplasticizer

ε: changing constraint value

MC: multiple-criteria

I. CHAPTER

1. Introduction

1.1. Justification

Since concrete is the most used material in construction, from a sustainability viewpoint reduction on concrete fabrication energy costs and CO_2 emissions are critical [1], [2]. As a consequence, new efforts are dedicated to partly replace cement with mineral admixtures (MAs) to help lower the total mix cost while lessening environmental damage.

In addition, more government institutions require that the modern constructions consider their environmental impact. One common requirement to contractors is to use recycled materials in constructions that are safe and robust to resist strong winds, high loads, and a long range of temperatures, as well as withstand natural hazards. As a consequence, research and development divisions of building companies have higher costs associated with the characterization of these materials. Also, new technologies require the development of high performance materials with specific characteristics. Often, the methodologies utilized are not based in proper statistical methodologies. Consequently, it takes longer to find appropriate results since more trials are generally needed when there is no known physical model that explains the phenomenon [3]. A statistical design of experiments (DOE) can be the only feasible alternative to characterize new cementitious materials [4]–[7]. DOE can help researchers find the desired results faster and, thus, in a more economically efficient manner. Some of the advantages of using DOE are that you can build a model that represent your system, predictions can be made in areas that there are not experimental data, the significant factors of the system can be identified, and so on. One disadvantage of using DOE, perhaps, is that the number of design points can increase too much when the number of factors increases. In our case, DOE can help develop high performance concrete containing recycled materials. In other words, this work intends to characterize, model, and optimize key performance measures of concrete containing Portland cement (PC), fly ash (FA), and nanosilica (nS).

A variety of DOE methodologies are available in the literature. Depending on the application, some methodologies are more suitable than others. In many cases, the factor levels considered in a process are independent from each other [8]. However, there are cases in which the selection of one factor level will affect directly the value or level of other factors. For example, if we consider a system with two factors: percentage of FA and percentage of PC; and we want to use 40% of FA in a cement mixture, consequently the other 60% will have to be PC to complete the 100% of the cement mixture. Also, if there are three mixture factors considered such as PC, FA, and nS; and we desire to use 20% of FA and 3% of nS, the percentage of PC will be 77%. As mentioned, in these cases the factor levels are related to each other. Hence, the use of a factorial design or a central composite design is inadequate. On the other hand, a mixture experiment design considers the system factors as the ingredients or components of the mixture [8]. In addition, the response variable is a combined result of the components considered.

This work implements a DOE for mixtures to determine the proportional amounts of each factor, i.e., PC, FA, nS, to evaluate in the cement mixture. These proportions are measured by considering the total cement weight required for the concrete mixture. Yet, before further considerations on the data treatment one needs to understand the mechanical behavior of the material. In particular, concrete has many physical and mechanical properties of interest. Since concrete final application defines the desired characteristics of concrete and the priority order given to them. Even so, there are some common concrete performance measures such as compressive strength, tensile strength, bulk density, and percentage of voids (porosity). In this work, first we evaluate the compressive strength of concrete. This is done by using a DOE for mixtures that provides a regression model for predicting this performance measure during the early age of concrete containing MAs. Then, more performance measures were considered as the concrete bulk density, percentage of voids, and compressive strength. This time a multiple-criteria optimization methodology was utilized in order to evaluate the different mixtures generated.

1.2. Objective

This work focuses primarily on the characterization of concrete containing MAs and its further compressive strength optimization. Subsequently, the optimal tradeoffs between compressive strength and material density shall be investigated. To this purpose the use of DOE, single criteria optimization, and multiple criteria optimization will be employed. It is envisioned that the contribution of this work results in a novel strategy to make decisions on the replacement of concrete components while taking into account the optimization of the mixture.

1.3. Literature Review

1.3.1. Supplementary Cementing Materials and nanoparticles of Silica

In the last decade, cement replacement such as supplementary cementing materials (SCM) in general, and FA and silica fume (SF) in particular, became of much interest [9], [10]. Unfortunately, because of its nature FA is the SCM with the highest variability in chemical composition, causing sometimes unpredictable results. Mixtures that contain FA are considered as eco-concrete mixtures, which are economically attractive and help reduce CO_2 emissions upon cement fabrication. To compensate for the detrimental effects of reducing the concrete compressive strength, alternatives such as addition of calcium directly during the burning coal process and using nS as an additive to the cement blend are being studied [11], [12]. Figure 1.1 illustrates the gain in compressive strength when nS is added to a PC with MAs mixture compared to the compressive strength of a conventional PC mixture (this graph was constructed from our experimental data).

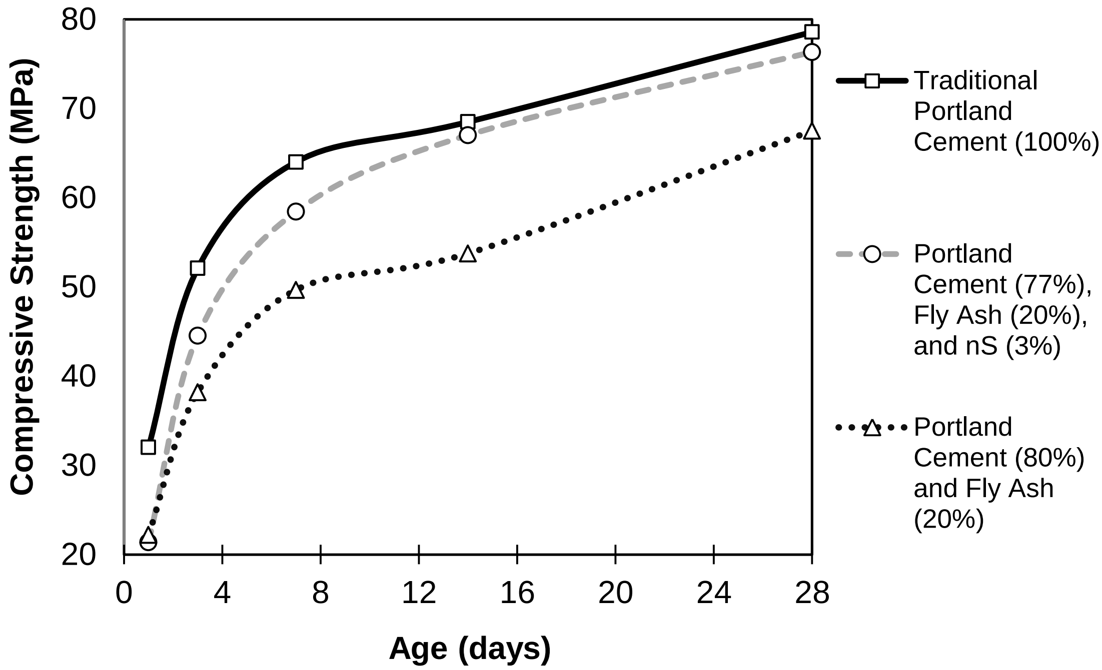

Figure 1.1 Compressive strength in mixtures bearing different proportions of cement as a function of the mixture age.

The use of nS in addition to raise the concrete compressive strength also accelerates the concrete hardening process, increases its density, reduces its porosity, and improves the binding among cement paste and aggregates [13]–[16]. However, it is not well known how much compressive strength is earned when specific amounts of nS are used.

After adding specific levels of FA and nS to concrete mixtures some researchers were able to analyze the resulting compressive strength for each combination of those levels [9]–[13], [15], [17]. However, that approach did not consider the possible interaction among the PC, FA, and nS added. Some researchers used linear regression models to make predictions on the compressive strength of the mixture as part of an observational study [9]. This approach allows identifying the significant terms including the interactions terms, however causality cannot be established.

To assess this, we deemed necessary to integrate a DOE to manipulate the factors in order to identify their effect on the compressive strength [4]–[7]. This strategy allows evaluating the use of these materials (FA and nS), studying their interaction, and may establish a relationship between the factors and response variable in the concrete mixtures. Hence, this work proposes a statistical design of experiments for mixtures to fully characterize the effect of FA and nS in concrete compressive strength at its early age.

1.3.2. Multiple Criteria Optimization

The decision making process is an important issue in the construction industry [18]. This industry has to deal with the environmental aspect and design factors at the same time. The majority of the elements related to this field are in conflicting aspects, since the designs that used recycled materials are not necessarily the more robust.

Often, research investigations related to concrete mixture report a breadth of physical and mechanical properties of the specimens. Some of them are fresh density, bulk density, slump, compressive strength, split tensile strength, flexural strength, percentage of voids, water absorption, shrinkage, consistency, among others [11], [16], [19]–[24]. Depending of the application, some performance measures are more important than others. For that reason, researchers just collect and analyze the performance measures of interest.

Different methodologies are utilized to independently analyze the results of compressive strength, density, and percentage of voids. Usually, regression models are used in order to predict the performance measures mentioned [6], [25]–[27]. Sometimes, neural networks are also employed to predict these concrete characteristics [6], [26]. In addition, different types of graphs are used to compare the characteristics of the mixtures. Although a visual representation of the results facilitates the comparison process, other statistical methodologies can be used to compare the mixtures from a mathematical viewpoint and not subjectively. Therefore, a variety of optimization approaches have been used to find the best possible solutions in a single objective [4], [28]–[33]. Final recommendations are made often based on each individual performance measures considered. Recommendations based on all the performance measures of interest to the user are more appropriate; when compared to just select a single solution according to the measured objective.

To address this situation, different approaches of multiple criteria optimization have been used. One of the methods is the TOPSIS-based Taguchi optimization to regulate the mixture proportions [34]. Similarly, the Taguchi off-line method was utilized to analyze the residual compressive strength of post-fire high performance concrete [35]. The ε-constraint method was utilized to optimize the design of the reinforced concrete frames [36]. Also, this method was used to resolve a multi-objective reliability-based optimum (MORBO) problem of pre-stressed concrete beams [37]. In order to optimize the high strength concrete parameters, a multi-objective optimization was solved by using a Genetic Algorithm (GA) employing weighted and hierarchical methods [26]. The desirability function approach was used to reinforce concrete with carbon nanofiber and polyvinyl alcohol and optimize several concrete properties [38]. Nevertheless, most of these methods require target values or decompose the multi-objective problem into a single objective optimization problem to find the optimal set. The methodology employed in this work does not involve any of the previously mentioned issues, and has been developed by the Applied Optimization Group at UPRM throughout the time [39]–[41]. Instead, it provides us the Pareto-optimal solution set just defining the objectives and its respective (maximization/minimization) directions.

1.4. Scope and General Organization of the Thesis

The scope of this thesis encompasses the use of different optimization strategies in order to analyze several concrete mixtures in terms of compressive strength at early age. A statistical design of experiments was employed to determine the mixture proportions to evaluate. In addition, as part of a second stage, we utilized multiple criteria optimization to evaluate different performance measures of the material. These physical and mechanical properties are bulk density, percentage of voids, and compressive strength.

II. CHAPTER

2. Design of Experiments and Optimization Strategies for Cement Mixtures Involving Portland Cement, Fly Ash, and Nanosilica

2.1. Introduction

The most common MAs–also known as supplementary cementing materials–that are often added to concrete mixtures are FA and SF [11]. FA is a manufacturing waste produced during coal burning and is the most frequently used SMC to replace PC in concrete mixtures [11]. Researchers found that after 90 days FA increases the strength and durability of concrete, and the resulting product is more environmentally-friendly and less expensive than cement [9], [11], [42], [43]. However, in some cases when FA class F is used as SCM, the material loses compressive strength at early age due to a slower reaction [42]. The FA physicochemical properties effect such slow reaction because it requires a pozzolanic reaction to form compounds that bear cementitious properties [42]. This reaction requires more days than the hydration process of the conventional mixes. In addition, a concrete mixture that contains SCM requires more curing days than conventional mixtures. The construction industry is fast paced and, for this reason, a concrete mixture with MAs translates into economic losses. This situation can represent more days to remove the woodwork that serves as support for the structure as the concrete dries and other ancillary costs.

When SCM is present, the “early age” scale can extend to more than 28 days, as it is usually considered for regular concrete with PC; for example, when fly ash is used, the early age can be considered to extend up to 56 days. However, due to the scope of the present work, for the ensuing experiment we shall call “early age” the first 28 days of curing.

In this first stage, the present work studies the strengthening of concrete during the early age to avoid accidents resulting from structure weakness by using nS to compensate for the loss of concrete compressive strength caused by the cement replacement. Additionally, this work proposes the alternative use of nS as an accelerator of the concrete hardening process, resulting in higher compressive strength at early age and long durability thereupon. The objective is, therefore, to shed more light on the understanding of compressive strength gains when adding nS to a concrete mixture using cement with MAs, as opposed to perfectly reproducing the behavior of a conventional mixture with just Portland cement.

2.2. Background

2.2.1. Statistical Design of Experiments (DOE)

Well-planned experiments play an important role in the characterization and optimization of processes; hence, the process of designing an experiment is critical. It requires time and knowledge to propose an experimental plan with foreseeable strengths and contingency actions that effectively leads to answer materials’ research questions.

An experiment can be defined as the manipulation of controllable variables of a system/process to measure their effect on responses of interest in such system [44]. As a consequence, there are different designs to conduct experiments. For example, the 2^k experiments evaluate k factors in two levels each one. These experiments are helpful as screening designs since they are useful to identify important factors in a system. Specifically, at the start of a study where there are a lot of factors that may be considered, a reduction on the number of factors to evaluate is necessary. However, when the response surface of the system under analysis is suspected or known to be non-linear, it is necessary to employ other types of designs.

Such is the case of this work where, due to the nature of the process, a design of experiments with mixtures was performed. Here, the factors or components of the mixture (i.e., PC, FA, and nS) depend on the values selected for the other components and the response is a combination of the proportions of each component [8]. Since each component of the cement mixture has both lower and upper control limits, a DOE with mixtures employing extreme vertices was selected. Figure 2.1 represents a mixture design with extreme vertices, where U_i and L_i are the upper and lower control limits, respectively.

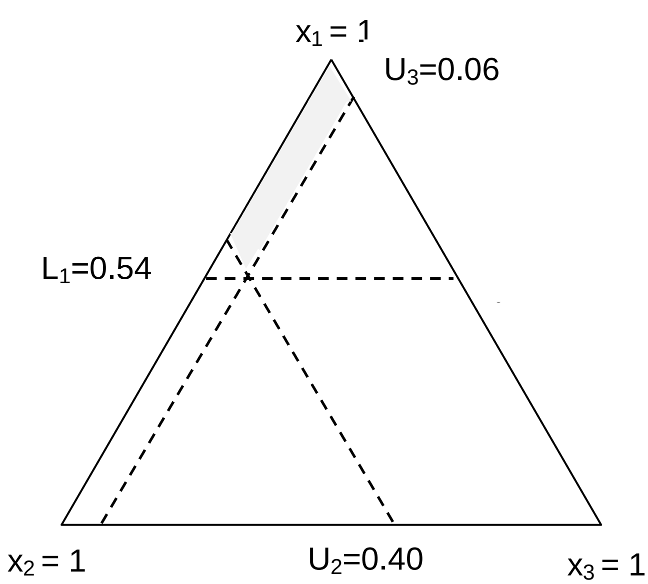

Figure 2.1 Example of a mixture experiment design with extreme vertices.

2.2.2. Single Objective Optimization

Optimization is a useful tool in decision making processes. Currently, there exists a variety of methods to optimize systems that can find the best system conditions or provide the researcher with a probability of being close to an optimum [45], [46]. The best known optimization method is, perhaps, the simplex, which is only applicable to linear problems [8], [44]. In a feasible problem, the simplex method tries to move from one corner point to a better corner point from the feasible space region given by the constraints until the optimum solution is found or declared to be unbound. A global optimal solution or a series of equivalent optimal solutions result from the application of the simplex method [45].

Since the objective function in this work–as explained later–is nonlinear, other optimization methods had to be employed. Optimization formulations were coded in Microsoft Excel ® and approached with the MS Solver through the Generalized Reduced Gradient (GRG2) Algorithm for nonlinear problems. This algorithm allows converging to solutions that meet all the constraints while using multi-starting points to improve the chances of finding a competitive solution. This process is an iterative method that utilizes the derivatives and gradients to search for the improvement of the objective function through the manipulation of the declared decision variables [47].

2.3. Methodology

2.3.1. Design of Experiment for Mixtures

The design of experiments for mixtures was used to study the effect of coarse and fine aggregate, water, and PC as components of the concrete mixture. Since the main interest has been the cement replacement, our work focused specifically on the cement mixture that is added to the final concrete mixture (Figure 2.2).

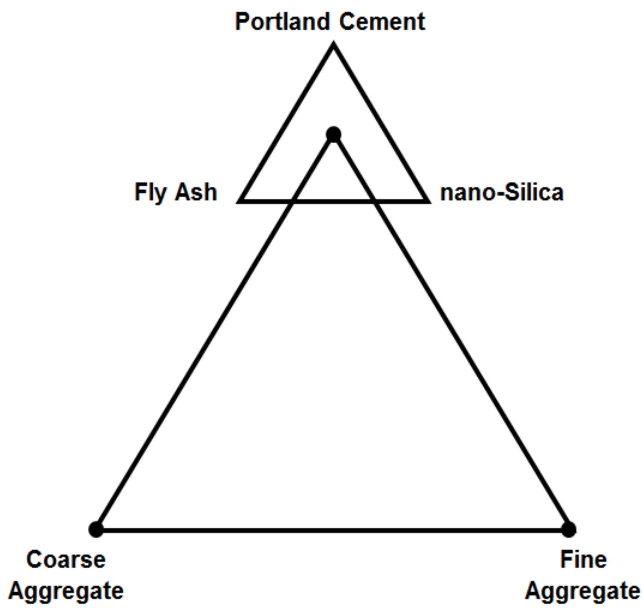

Figure 2.2 Experiment design with mixtures including the cement mix within the concrete mixture.

As previously mentioned, the design uses PC, FA, and nS as cement mixture components where the sum of all component proportions should equal one. The lower and upper experimental limits of each component were as follows:

a) FA varied from 0% to 40%, which is a common upper limit in industrial practice [48]–[50].

b) The nS amount was varied from 0% to 6% since more than 6% is not recommended because it may lead to chemical incompatibilities due to dispersion problems [14].
c) The PC level was varied from 54% to 100% (Table 2.1).

Therefore, a design of experiments based on mixtures with extreme vertices was considered [8]. The feasible region can be observed in Figure 2.3.

Table 2.1 Lower and upper proportion limits for the cement mixture components.

Mixture Components	Lower Limit	Upper Limit
Portland cement	54%	100%
Fly ash	0%	40%
Nanosilica	0%	6%

Additionally, the water-to-binder (w/b) ratio was included in the experiment as an external factor or decision variable in two levels: 0.3 (low) and 0.5 (high); this allowed varying the amount of water in the mixture. These levels reflected the limits usually found in the industrial fabrication of structural concrete [17]. The points in the experimental design prescribe the proportions for each mixture to be evaluated (Figure 2.3). Three replicates were measured on each design point while the total number of design points considering the w/b factor was eighteen.

The number of replicates was predetermined to three in this experiment according to the literature [51]. Afterwards, that sample size was evaluated statistically through the use of an operating characteristic curve because the standard followed do not specify the power and size difference that the experiment will have.

Equation 1 presents the cubic regression model fitted to study the compressive strength, i.e., the response variable, for different days.

$$Y_t = \hat{\beta}_1 PC + \hat{\beta}_2 FA + \hat{\beta}_3 nS + \hat{\beta}_4 PC * FA + \hat{\beta}_5 PC * nS + \hat{\beta}_6 FA * nS + \hat{\beta}_7 PC * FA * nS + \hat{\beta}_8 PC * \frac{w}{b} + \hat{\beta}_9 FA * \frac{w}{b} + \hat{\beta}_{10} nS * \frac{w}{b} + \hat{\beta}_{11} PC * FA * \frac{w}{b} + \hat{\beta}_{12} PC * nS * \frac{w}{b} + \hat{\beta}_{13} FA * nS * \frac{w}{b} + \hat{\beta}_{14} PC * FA * nS * \frac{w}{b} \tag{1}$$

where PC, FA, and nS represent the Portland cement, fly ash, and nanosilica proportions, respectively, added to the concrete mixture; w/b is the value of water-to-binder ratio used in the mixture, and Y_t is the compressive strength measured in MPa on the t-th day of age.

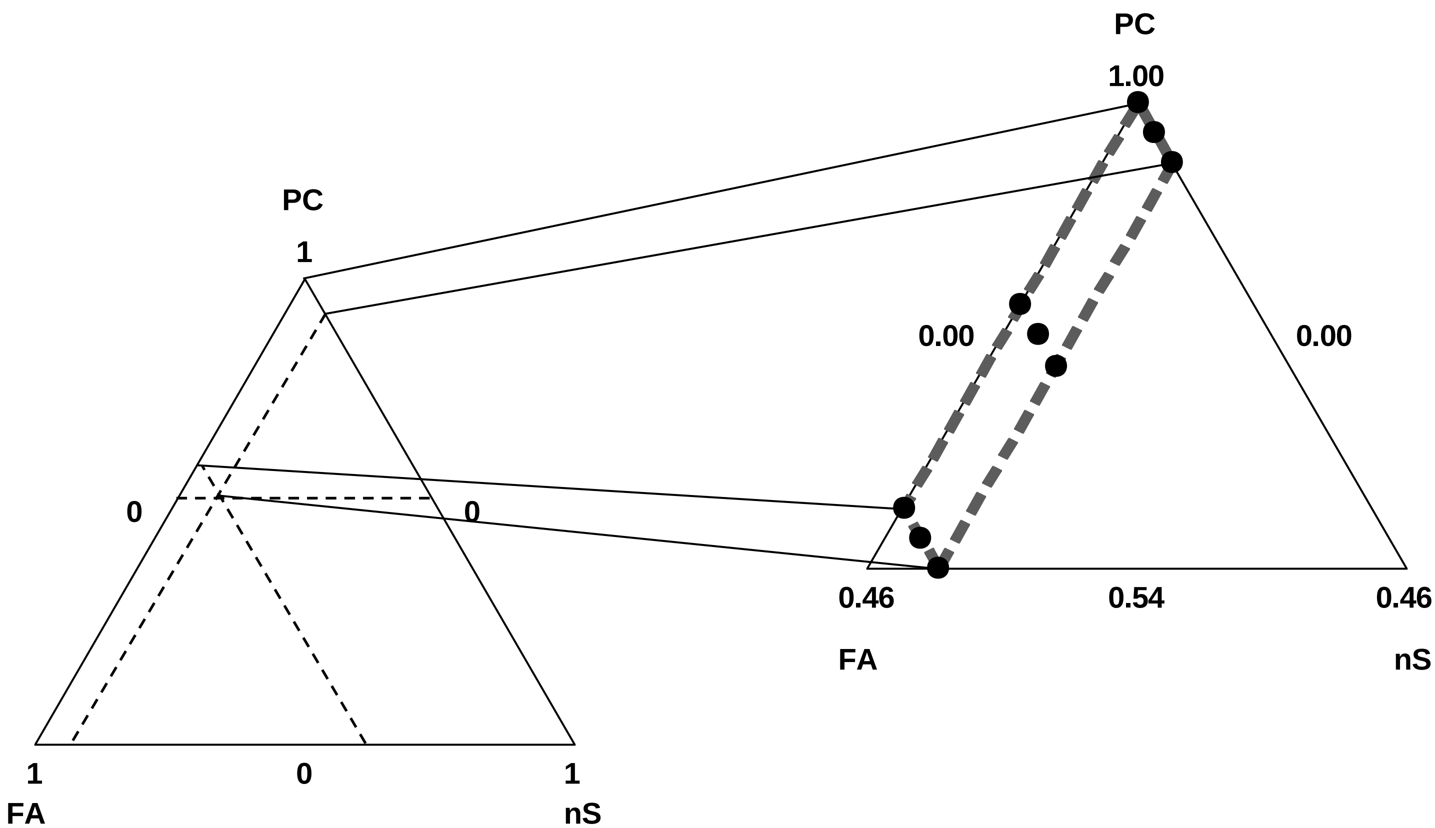

Figure 2.3 Mixture proportions (design points) evaluated within the constrained experimental region.

2.3.2. Experimental Conditions

A preliminary granulometry study allowed establishing the experimental proportions of the aggregates: 30% of limestone, 35% of processed-aggregate, and 35% of clean beach sand. As mentioned, PC type I was utilized to prepare the mixtures. Furthermore, mixture behavior (i.e., segregation, bleeding, slump loss, and consistency) was taken into account to determine the quantity of polycarboxylate superplasticizer (SP) necessary for each mixture.

Additionally, while concrete strength upon the hardening state is important, one cannot disregard the workability during the fresh state. When nS is added to the mixture, additional water is required [14]. As a consequence, it was important to study and analyze the behavior and workability of the mixture during its fresh state when two w/b ratio were utilized. Also, the two w/b ratios allowed observing the reactability of the materials under different aqueous states. In addition to water, SP was needed to maintain the workability of the mixture for a longer time. The mixture workability was assessed in the slump analysis of the mixtures.

2.3.3. Materials

The materials utilized in this work are listed and described in this section. The origin and suppliers of these materials were the same during the execution of this first phase of the experiment to minimize the dispersion due to slight variations in chemical composition and the nature of the materials used.

Aggregates

Limestone was used as coarse aggregate and its maximum diameter was 9.5 mm. In addition, the processed-aggregate had a maximum diameter of 4.8 mm. The fineness modulus of the fine aggregate, i.e. beach sand, was 2.02.

Table 2.2 Properties of the aggregates.

Aggregate	Apparent Specific Gravity	Specific Gravity (Oven-dry)	Specific Gravity (SSD)	Absorption (%)	Unit Weight (kg/m^3)
Limestone	2.6	2.4	2.5	3.5	1510
Processed-aggregate	2.5	2.0	2.2	9.0	1591
Beach Sand	2.7	2.5	2.6	3.1	1623

Portland Cement

The PC Type I utilized to prepare the mixtures had a specific gravity of 2.9.

Fly Ash

The FA class F used for the mixtures possessed a specific gravity of 2.22.

Nanosilica

The nS used in this work was originally suspended in an aqueous solution, with a mean particle size of 23.22 nm. This was provided by Nissan Chemical Industries.

Superplasticizer

The polycarboxylate superplasticizer used was the ADVA 575 and was obtained from Instron in PR.

Water

The water used to prepare the mixtures was tap water at room temperature.

2.3.4. Fabrication and Testing Procedure

A Blakeslee mixer machine was utilized to mix the concrete components (Figure 2.4 and Figure 2.5). The aggregates were first introduced in the mixer for 0.5 min at 60 rpm followed by half of the required water. PC was dry-mixed with FA (when necessary) and then added to the mixer for 0.5 min at 60 rpm. The nS and SP were diluted in water in order to obtain a uniform distribution of the particles throughout the mixture and added to the mixer (when used) for 5 min at 120 rpm. Fifteen cylinders were filled using the rodding method [51]. The dimensions of the test cylinders prepared for each mixture had 50 mm in diameter and 100 mm in length [52](Figure 2.6).

Figure 2.4 Blakeslee Mixer Machine utilized.

Figure 2.5 Fresh mixture example.

Figure 2.6 Concrete cylinders filled with eight mixtures.

Three cylinders were tested for compressive strength at 1, 3, 7, 14, and 28 days of curing (Figure 2.7 and Figure 2.8). The compression tests were performed in a 3000 kN FORNEY Universal Tester machine according to American Society for Testing and Materials (ASTM) International standards [53]. The first three cylinders were demolded and then tested. The other ones were placed in limewater until tested at normal curing conditions (20-23ºC and relative humidity=100%). The temperature (23-25ºC) in the experiment was deemed constant.

Figure 2.7 Concrete cylinder in the 3000 kN FORNEY Universal Tester machine.

Figure 2.8 Concrete cylinder after the compression test.

2.4. DOE Results and Discussion

The mixtures with higher compressive strength were the ones bearing w/b ratio of 0.3 (Figure 2.9); the range in compressive strength obtained was 11.51 MPa (at 1day) to 86.32 MPa (at 28 days). The less resistant ones were those with a w/b ratio of 0.5 (Figure 2.10), ranging from 2.79 MPa (at 1 day) to 49.85 MPa (at 28 days). The individual mixtures with higher compressive strength were those containing only PC and nS. These two mixtures, that is mix 13 and 12, exceeded the control one (mix 7), which only had PC; all these mixtures contained a w/b of 0.3 (Table 2.3). This behavior remained the same for both w/b ratio levels. However, since the interest of this work was the cement replacement by FA, these mixtures were not considered practical (out of scope). In other words, a practical mixture is considered to be a mixture that contains the manufacturing waste FA with the highest compressive strength. Mix number 11 and 15 could be mentioned as mixtures of interest. Some characteristics of these mixtures are that they contain FA, include silica nanoparticles, exceed 70 MPa after day 28, and have a w/b ratio of 0.3.

Table 2.3 Average compressive strength of the three replicates in each testing day.

	Mix Num.	Portland Cement	Fly Ash	nano-Silica	water/ binder	Compressive Strength									
						Y_1 (MPa)	St. Dev. (MPa)	Y_3 (MPa)	St. Dev. (MPa)	Y_7 (MPa)	St. Dev. (MPa)	Y_{14} (MPa)	St. Dev. (MPa)	Y_{28} (MPa)	St. Dev. (MPa)
	1	0.94	0.00	0.06	0.5	14.98	0.79	30.45	1.81	47.38	1.15	48.56	0.78	48.81	1.24
	2	0.80	0.20	0.00	0.3	22.20	0.62	38.20	2.00	49.67	1.95	53.76	1.03	67.50	3.37
	3	0.54	0.40	0.06	0.5	4.25	0.35	12.90	1.47	18.33	3.80	20.31	2.70	26.90	2.05
	4	0.57	0.40	0.03	0.5	2.98	0.16	7.83	0.27	15.67	0.83	16.62	1.80	21.49	0.67
	5	0.60	0.40	0.00	0.5	2.98	0.11	6.19	0.11	10.00	0.52	14.59	1.11	19.87	0.20
	6	1.00	0.00	0.00	0.5	8.41	0.49	19.27	0.36	27.04	0.09	27.90	0.61	32.06	1.86
Control	7	1.00	0.00	0.00	0.3	32.03	0.84	52.09	2.47	64.01	3.70	68.50	1.22	78.58	1.66
	8	0.60	0.40	0.00	0.3	16.46	0.70	23.68	0.76	32.11	1.26	43.70	2.42	54.70	2.66
	9	0.57	0.40	0.03	0.3	16.40	0.28	28.14	0.57	45.77	0.98	51.19	2.63	60.94	2.54
	10	0.80	0.20	0.00	0.5	5.62	0.16	12.39	0.16	16.87	0.26	21.65	1.98	28.89	0.61
	11	0.74	0.20	0.06	0.3	24.92	0.71	51.52	1.53	63.90	1.59	68.44	2.90	75.31	1.39
	12	0.97	0.00	0.03	0.3	30.59	0.08	55.65	1.18	66.99	2.80	75.05	2.19	80.04	0.54
Out of scope	13	0.94	0.00	0.06	0.3	30.56	0.52	58.58	2.55	73.15	3.02	80.51	1.53	84.43	2.55
	14	0.97	0.00	0.03	0.5	11.90	0.24	25.79	0.45	33.08	0.71	37.68	0.61	41.92	1.04
Mix of interest	15	0.77	0.20	0.03	0.3	21.35	0.02	44.52	0.82	58.44	1.69	67.02	2.05	76.34	3.32
	16	0.54	0.40	0.06	0.3	12.24	0.64	36.63	0.55	52.42	1.59	58.24	0.85	64.78	3.04
	17	0.77	0.20	0.03	0.5	6.46	0.07	16.60	0.85	25.14	0.42	31.88	1.15	31.66	1.70
	18	0.74	0.20	0.06	0.5	6.94	0.54	18.73	1.24	30.23	0.18	33.08	1.00	37.43	1.62

Y_t correspond to the compressive strength measurement taken in day *t*.

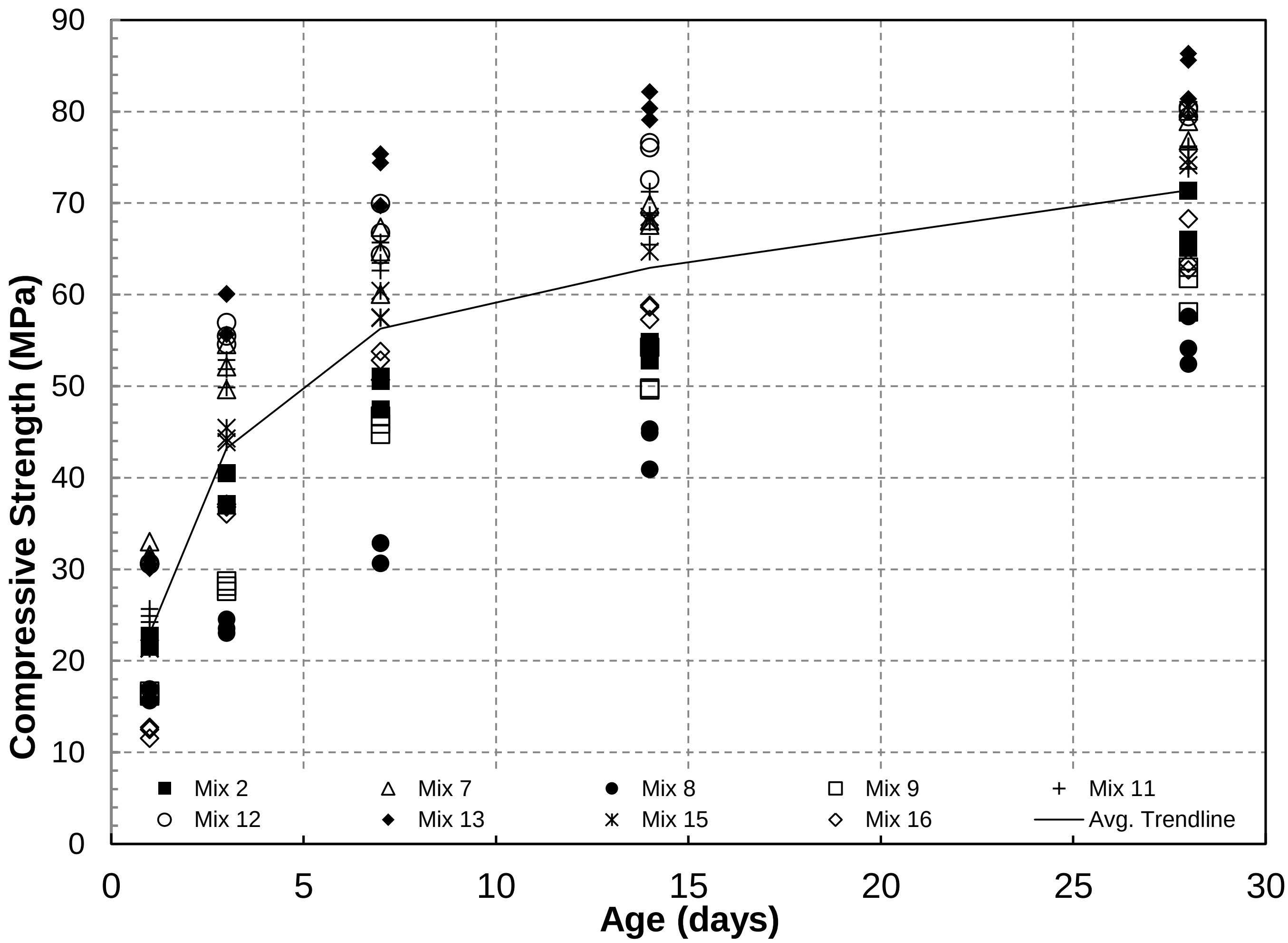

Figure 2.9 Compressive strength of concrete cylinders fabricated with a w/b ratio of 0.3 after curing.

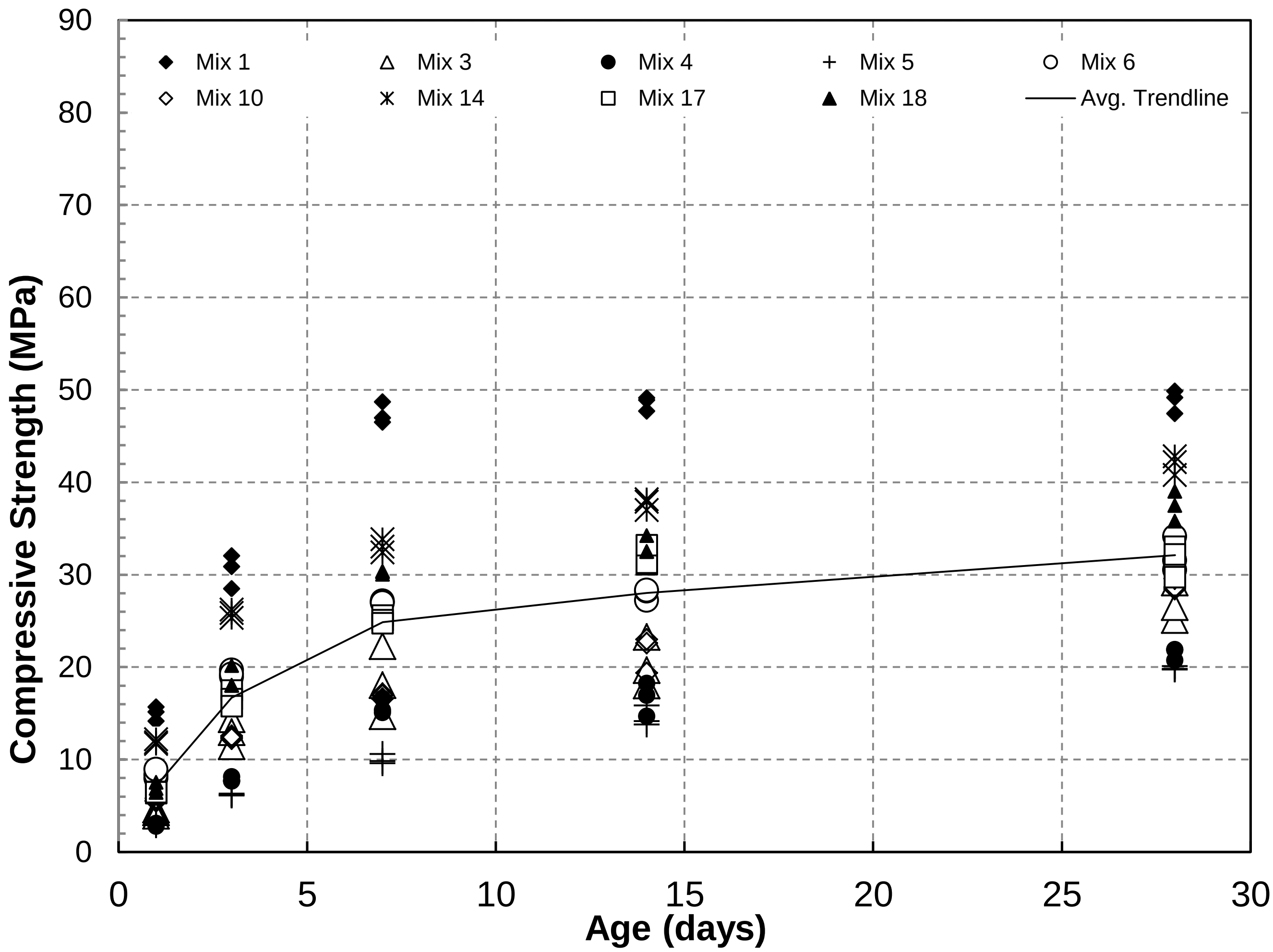

Figure 2.10 Compressive strength of concrete cylinders fabricated with a with w/b ratio of 0.5 after curing.

On the other hand, the standard deviation values between the three replicates were acceptable. These values were below 3.80 MPa (Table 2.3); and in the construction industry differences in mixtures are considered more than approximately 7 MPa (1,000 psi). Nevertheless, a Bartlett test for the standard deviation values was used to verify if the variability reported by the different levels of testing days was the same across the concrete age evaluated (Figure 2.11). The significance level selected was 0.05; the p-value obtained from the test was below this value (0.000). Therefore, there is a difference in terms of the variability reported by testing day. According to the graph, the standard deviation values from day 1 were smaller than the others.

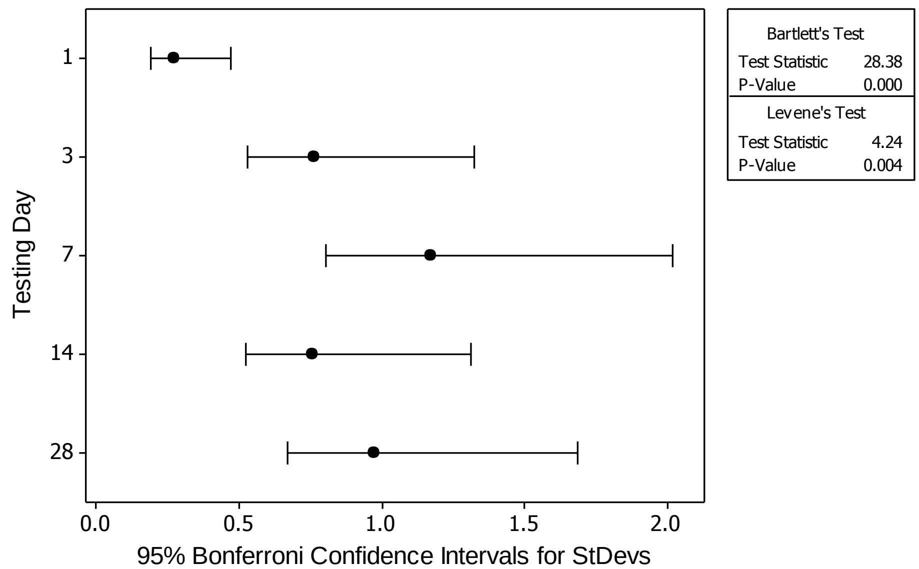

Figure 2.11 Bartlett test performed to the standard deviation values from each testing day.

After completing the mixture analysis, we identified the interaction terms that significantly affected the response variable as a function of the age in days. To this purpose, we used Minitab ® 16.2.20 to analyze the DOE results. Y_1 in our experiments corresponded to the compressive strength measurements taken in day 1, Y_3 for those in day 3 and so on. The regression models obtained for compressive strength are presented in the following tables. A new set of components were defined in order to make easier the model fitting over the constrained region, these components are known as pseudocomponents [8]. They were utilized to reduce the high levels of multicollinearity that usually have the constrained design spaces. Also the pseudocomponents help to reduce the inflated variance of the coefficients estimators.

According to a constrained DOE for mixtures [8], the sum of the components proportion equals 1 (Equation 2).

$$x_1 + x_2 + \cdots + x_q = 1$$

$$L_i \leq x_i \leq U_i, \quad i = 1,2, \dots, q \tag{2}$$

where the lower bound constraint $L_i \geq 0$ and the upper bound constraint $U_i \leq 1$ for all q that is the number of components of the cement mixture (PC, FA, and nS).

We used Equations 3 and 4 to convert the original proportions x_i to pseudocomponents.

$$X_i = \frac{x_i - L_i}{1 - L} \tag{3}$$

$$L = \sum_{i=1}^{q} L_i < 1, \tag{4}$$

where X_i is the pseudocomponent and L is the sum the lower constraints.

The regression models obtained from Minitab for each testing day are presented in the following tables: Table 2.4,

Table 2.5,

Table 2.6, Table 2.7, and Table 2.8) with their respective p-values for each interaction terms. The statistical level of significance was set at α=0.10 for this specific analysis. The terms that were statistically significant in all the models were the interactions between PC and w/b ratio and FA with w/b ratio. However, most of the interactions became statistically significant at least one time within the age of concrete evaluated. The only term that was not statistically significant during the concrete age evaluated was the interaction between nS and w/b. In order to decide if it was appropriate to use a model without this term, the adequacy of the models was verified. First, the analyses were performed on the regression models containing all the terms and then the interaction between nS and w/b was removed from the models.

Table 2.4 Estimated regression coefficients for Y_1 in pseudocomponents.

Term	Coef	SE Coef	T	P	VIF
PC	20.3	0.300	*	*	3.1
FA	9.5	0.468	*	*	6.3
nS	101.9	45.995	*	*	1374.7
PC*FA	-8.1	1.841	-4.39	0.000	5.5
PC*nS	-71.7	52.946	-1.35	0.183	596.1
FA*nS	-115.2	53.517	-2.15	0.037	586.3
PC*FA*nS	64.5	21.768	2.96	0.005	4.0
PC*w/b	-11.8	0.300	-39.49	0.000	3.1
FA*w/b	-7.6	0.468	-16.13	0.000	6.3
nS*w/b	-66.6	45.995	-1.45	0.155	1374.7
PC*FA*w/b	8.6	1.841	4.64	0.000	5.5
PC*nS*w/b	99.0	52.946	1.87	0.069	596.1
FA*nS*w/b	96.3	53.517	1.80	0.080	586.3
PC*FA*nS*w/b	-172.7	21.768	-7.94	0.000	4.0

Table 2.5 Estimated regression coefficients for Y_3 in pseudocomponents.

Term	Coef	SE Coef	T	P	VIF
PC	35.9	0.541	*	*	3.1
FA	10.8	0.846	*	*	6.3
nS	167.6	83.043	*	*	1374.7
PC*FA	2.6	3.324	0.79	0.434	5.5
PC*nS	-72.4	95.592	-0.76	0.453	596.1
FA*nS	-61.0	96.623	-0.63	0.532	586.3
PC*FA*nS	4.9	39.301	0.12	0.902	4.0
PC*w/b	-16.5	0.541	-30.53	0.000	3.1
FA*w/b	-7.4	0.846	-8.80	0.000	6.3
nS*w/b	-123.4	83.043	-1.49	0.145	1374.7
PC*FA*w/b	-1.0	3.324	-0.31	0.759	5.5
PC*nS*w/b	143.5	95.592	1.50	0.141	596.1
FA*nS*w/b	94.3	96.623	0.98	0.335	586.3
PC*FA*nS*w/b	-123.9	39.301	-3.15	0.003	4.0

Table 2.6 Estimated regression coefficients for Y_7 in pseudocomponents.

Term	Coef	SE Coef	T	P	VIF
PC	44.6	0.863	*	*	3.1
FA	18.4	1.349	*	*	6.3
nS	69.5	132.489	*	*	1374.7
PC*FA	0.9	5.303	0.18	0.860	5.5
PC*nS	98.9	152.511	0.65	0.520	596.1
FA*nS	96.2	154.156	0.62	0.536	586.3
PC*FA*nS	2.9	62.702	0.05	0.964	4.0
PC*w/b	-18.6	0.863	-21.62	0.000	3.1
FA*w/b	-9.1	1.349	-6.75	0.000	6.3
nS*w/b	178.0	132.489	1.34	0.187	1374.7
PC*FA*w/b	-6.8	5.303	-1.28	0.207	5.5
PC*nS*w/b	-176.9	152.511	-1.16	0.253	596.1
FA*nS*w/b	-285.9	154.156	-1.85	0.071	586.3
PC*FA*nS*w/b	-7.8	62.702	-0.12	0.901	4.0

Table 2.7 Estimated regression coefficients for Y_{14} in pseudocomponents.

Term	Coef	SE Coef	T	P	VIF
PC	47.6	0.844	*	*	3.1
FA	25.0	1.321	*	*	6.3
nS	-164.6	129.698	*	*	1374.7
PC*FA	4.4	5.191	0.85	0.398	5.5
PC*nS	388.2	149.298	2.60	0.013	596.1
FA*nS	337.9	150.908	2.24	0.031	586.3
PC*FA*nS	-8.5	61.381	-0.14	0.890	4.0
PC*w/b	-20.3	0.844	-24.06	0.000	3.1
FA*w/b	-14.5	1.321	-10.98	0.000	6.3
nS*w/b	110.4	129.698	0.85	0.400	1374.7
PC*FA*w/b	6.9	5.191	1.32	0.193	5.5
PC*nS*w/b	-112.3	149.298	-0.75	0.456	596.1
FA*nS*w/b	-182.5	150.908	-1.21	0.234	586.3
PC*FA*nS*w/b	-62.7	61.381	-1.02	0.313	4.0

Table 2.8 Estimated regression coefficients for Y_{28} in pseudocomponents.

Term	Coef	SE Coef	T	P	VIF
PC	55.1	0.871	*	*	3.1
FA	32.6	1.363	*	*	6.3
nS	21.0	133.856	*	*	1374.7
PC*FA	13.4	5.358	2.50	0.017	5.5
PC*nS	139.0	154.084	0.90	0.372	596.1
FA*nS	128.1	155.746	0.82	0.416	586.3
PC*FA*nS	-71.6	63.349	-1.13	0.265	4.0
PC*w/b	-22.5	0.871	-25.84	0.000	3.1
FA*w/b	-17.0	1.363	-12.44	0.000	6.3
nS*w/b	213.6	133.856	1.60	0.118	1374.7
PC*FA*w/b	0.9	5.358	0.17	0.863	5.5
PC*nS*w/b	-222.3	154.084	-1.44	0.157	596.1
FA*nS*w/b	-282.9	155.746	-1.82	0.077	586.3
PC*FA*nS*w/b	-81.6	63.349	-1.29	0.205	4.0

In order to study the adequacy of the models, some assumptions of regression analysis have to be checked. This validation is important since violations to these assumptions can result in an unstable model [54]. Therefore a normality test, equal variances test, and independence test were performed to the model residuals to verify the model adequacy. The residual analysis for the regression models containing all the terms shows that all the assumptions were satisfied (Table 2.9). The statistical test used to evaluate the residuals normality was the Kolmogorov-Smirnov. In addition, the Runs test was utilized to evaluate the independence of the residuals. Finally, Bartlett’s test was employed as the test for equal variances. All p-values obtained were above the chosen significance level (0.05); therefore the basic assumptions were satisfied.

Table 2.9 Model adequacy tests for residuals.

Residuals for:	Normality Test	Independence Test	Test for Equal Variances
	Kolmogorov-Smirnov	Runs Test	Bartlett's Test
	p-value	p-value	p-value
Y_1	0.146	0.575	0.678
Y_3	0.150	0.101	0.929
Y_7	0.150	0.101	0.988
Y_{14}	0.150	0.791	0.999
Y_{28}	0.150	0.155	1.000

The values of standard deviation obtained are acceptable in the scale evaluated, approximately ± 2 MPa (Table 2.10). The variability of the compressive strength is well explained by the model considered since the values of all the R-square, R-square predicted, and R-square adjusted are greater than 98.23% (Table 2.10). Consequently, the cubic regression model is useful to predict the average concrete compressive strength at the different ages evaluated.

Table 2.10 Summary of the variation and adjustment of the models.

Model	Standard Deviation	Model Adjustment		
	S	R-Sq	R-Sq(pred)	R-Sq(adj)
Y_1	0.768	99.53%	99.15%	99.37%
Y_3	1.386	99.48%	99.01%	99.31%
Y_7	2.211	99.04%	98.23%	98.73%
Y_{14}	2.164	99.18%	98.56%	98.92%
Y_{28}	2.234	99.22%	98.57%	98.96%

On the other hand, the adequacy analyses to the regression models after removing the interaction between nS and w/b from the models are presented in Table 2.11. The reduced regression models obtained from Minitab are presented in Appendix 2. In the normality test for the reduced models, the resulting p-value for Y_7 fell below the significant level established (0.05). Consequently, the residuals are not normally distributed implicating that the model can be underfitted. Therefore, the previous model can be considered reasonable because it adequately explains the data variability satisfying the basic assumptions. This fact supported our decision to keep all the terms in the regression models.

Table 2.11 Model adequacy tests for models without the insignificant term.

Residuals for:	Normality Test	Independence Test	Test for Equal Variances
	Kolmogorov-Smirnov	Runs Test	Bartlett's Test
	P-value	P-value	P-value
Y_1	0.049	0.415	0.678
Y_3	0.150	0.276	0.929
Y_7	0.150	0.589	0.988
Y_{14}	0.150	0.431	0.999
Y_{28}	0.150	0.783	1.000

After removing the insignificant term, the R-square's of the models are above 98.24% (Table 2.12). This means that these models can predict well the compressive strength of the mixtures evaluated. The standard deviations of the models are almost the same than the models with all the terms. However, the models that included all the terms were kept and used from here on since all the adequacy tests were acceptable.

Table 2.12 Adjustment of the models without the insignificant term.

Model	Standard Deviation	Model Adjustment		
	S	R-Sq	R-Sq(pred)	R-Sq(adj)
Y_1	0.778	99.50%	99.16%	99.36%
Y_3	1.406	99.45%	99.00%	99.29%
Y_7	2.232	99.00%	98.24%	98.70%
Y_{14}	2.157	99.17%	98.61%	98.92%
Y_{28}	2.275	99.17%	98.56%	98.92%

The correlation between the testing days was calculated to evaluate whether the relationship between them could be detected. All the correlation values were close to 1, which means that there existed a positive linear relationship among all the testing days (Table 2.13). These results suggested that the specimens of mixtures bearing higher compressive strength at day 7, for example, would also possess higher compressive strength at day 28 too. Moreover, specimens of mixtures with lower compressive strength at day 7, for example, will be maintained lower for longer ages.

Table 2.13 Correlation among testing days.

Correlations	Y_1	Y_3	Y_7	Y_{14}
Y_3	0.961	-	-	-
Y_7	0.937	0.983	-	-
Y_{14}	0.943	0.980	0.987	-
Y_{28}	0.949	0.967	0.968	0.982

2.5. Optimization Formulation

An optimization problem of maximizing concrete compressive strength was formulated in MS Solver, an optimization add-on tool available Microsoft Excel ®. This is intended to search for an optimal mixture that would satisfy all the restrictions and, simultaneously, be a practical mixture utilizing cement replacement. First, the data was divided in two groups (for every single mixture) with distinct behavior: before and after 7 days of age. During the first period, maturity of the concrete compressive strength increases rapidly, while in the latter such strength increases at a slower pace. A linear fit for the experimental data on days 1, 3, and 7 (group 1) was obtained for each mixture. Another linear model for the datasets at 7, 14, and 28 days (group 2) was also obtained. This analysis provided the slope and intercept of each straight line model for each mixture (Figure 2.12). Slope 1 and intercept 1 represented the fit for group 1; slope 2 and intercept 2 the fit for group 2 (Table 2.14). Since the interest of this work was to obtain the highest value of compressive strength at early age, higher values of slopes and intercepts were convenient. The same form of the cubic regression models showed before were utilized to represent this time the slope and intercept values as functions of the mixture proportions. Linear fits were utilized since our purpose was to identify the mixtures with higher compressive strength and not to replicate the behavior of those mixtures.

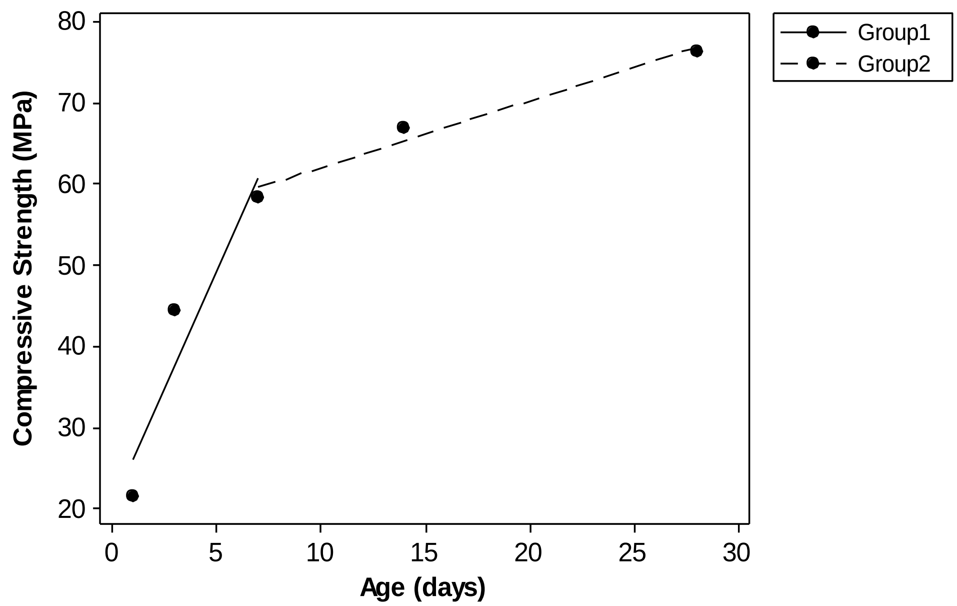

Figure 2.12 Mixture growth divided in two linear segments.

Table 2.14 Intercept and slope values for group 1 and 2.

Mix Number	Group 1: Y_1-Y_7		Group 2: Y_7-Y_{28}	
	Intercept1	Slope1	Intercept2	Slope2
1	11.75	5.232	47.25	0.06121
2	20.8	4.333	42.79	0.8682
3	3.745	2.205	15.03	0.4172
4	1.146	2.094	13.24	0.287
5	2.213	1.139	7.36	0.4567
6	7.466	2.938	24.96	0.2474
7	31.06	4.994	58.97	0.6976
8	14.78	2.537	26.61	1.034
9	12.41	4.826	40.9	0.7186
10	5.146	1.767	13.25	0.5645
11	24.74	6.011	60.47	0.5359
12	30.52	5.606	64.5	0.5832
13	29.88	6.606	71.19	0.5001
14	11.54	3.286	30.96	0.404
15	20.18	5.797	53.78	0.8254
16	10.65	6.305	49.15	0.5709
17	5.163	2.974	25.25	0.2637
18	4.928	3.738	28.06	0.3379

Afterwards, the regression model of Y_7, Y_{28}, and slope 1 were used in the solver to verify whether the suggested mixture proportions maximizing the compressive strength were the same. In this case, slope 1 was selected because the expectation was to increase it to achieve higher compressive strength. Regression models for Y_7 and Y_{28} were selected because the search seeks for a mixture with replacement of cement by FA that has the highest compressive strength in days 7 and 28.

Optimization problem:

Find PC, FA, nS, w/b to maximize Equation 5 satisfying the constraints given in Equations 6 through 12:

$$\mathrm{Y_i} = \hat{\beta}_1\mathrm{PC} + \hat{\beta}_2\mathrm{FA} + \hat{\beta}_3\mathrm{nS} + \hat{\beta}_4\mathrm{PC} * \mathrm{FA} + \hat{\beta}_5\mathrm{PC} * \mathrm{nS} + \hat{\beta}_6\mathrm{FA} * \mathrm{nS} + \hat{\beta}_7\mathrm{PC} * \mathrm{FA} * \mathrm{nS} + \hat{\beta}_8\mathrm{PC} * \frac{\mathrm{w}}{\mathrm{b}} + \hat{\beta}_9\mathrm{FA} * \frac{\mathrm{w}}{\mathrm{b}} + \hat{\beta}_{10}\mathrm{nS} * \frac{\mathrm{w}}{\mathrm{b}} + \hat{\beta}_{11}\mathrm{PC} * \mathrm{FA} * \frac{\mathrm{w}}{\mathrm{b}} + \hat{\beta}_{12}\mathrm{PC} * \mathrm{nS} * \frac{\mathrm{w}}{\mathrm{b}} + \hat{\beta}_{13}\mathrm{FA} * \mathrm{nS} * \frac{\mathrm{w}}{\mathrm{b}} + \hat{\beta}_{14}\mathrm{PC} * \mathrm{FA} * \mathrm{nS} * \frac{\mathrm{w}}{\mathrm{b}} \tag{5}$$

Subject to:

$$0.54 \le PC \le 1 \tag{6}$$

$$0 \le FA \le 0.40 \tag{7}$$

$$0 \le nS \le 0.06 \tag{8}$$

Components' Restrictions

$$PC + FA + nS = 1 \tag{9}$$

Convexity

$$w\ /\ b = 0.3Z_1 + 0.5Z_2 \tag{10}$$

$$Z_1 + Z_2 = 1 \tag{11}$$

$$Z_1, Z_2\ as\ binary\ variables \tag{12}$$

Change of Variable

where PC, FA, and nS are the proportions of Portland cement, fly ash and nanosilica respectively; w/b is the water to binder ratio; Z_1 and Z_2 are used to restrict the values of w/b to those considered in the experiment.

2.6. Optimization Results and Discussion

The results show that the three optimization formulations for slope 1, Y_7, and Y_{28} converged almost to the same proportions for each mixture component; hence, if one of them is maximized, the others will be maximized too. However, the proportions suggested correspond to an out of scope mixture with 94% of PC, 6% of nS, and 0% of FA. Therefore, the regression model of Y_7 was selected to maximize the concrete compressive strength but this time forcing the model to include some proportion of fly ash to the mixture for being of interest to the research. The constraint of FA greater than 0 was modified by FA greater than a given value of epsilon (ε), set at 0.00, 0.10, 0.20, 0.30, and 0.40. Then the component proportions found through the optimization procedure were recorded as the ones that maximized the response variable (Table 2.15 and Figure 2.13).

Table 2.15 Optimization results varying the lower constraint of FA.

Variation of Fly Ash	ε=	**0**	**0.10**	**0.20**	**0.30**	**0.40**
Optimizer Value (MPa)	Z=	**72.09**	**68.63**	**64.31**	**59.14**	**53.10**
Experimental Value (MPa)	Z=	**73.15**	**-**	**63.90**	**-**	**52.42**
Decision Variables in Proportions	PC=	0.94	0.84	0.74	0.64	0.54
	FA=	0.00	0.10	0.20	0.30	0.40
	nS=	0.06	0.06	0.06	0.06	0.06
	w/b=	0.3	0.3	0.3	0.3	0.3
Percentage of loss of Compressive Strength		-	4.8%	10.8%	18.0%	26.3%

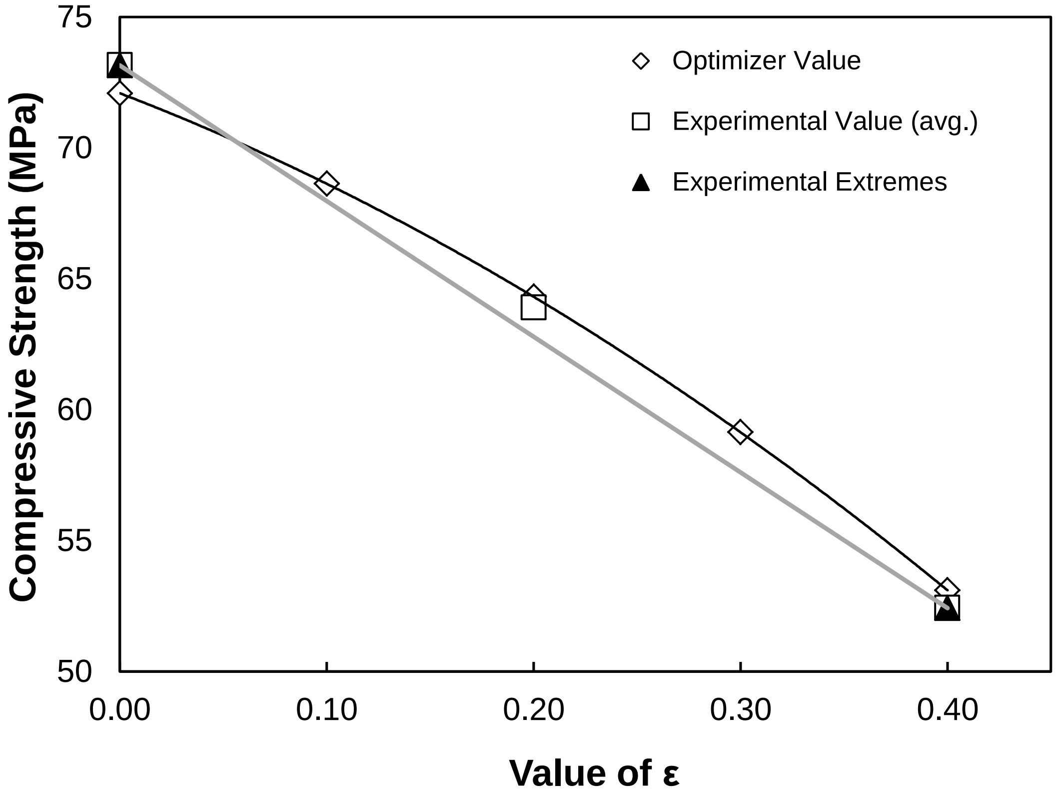

Figure 2.13 Variation of concrete compressive strength as a function of the amount of FA (nS is constant at 0.06).

This analysis demonstrated how the optimization procedure always selected the lowest value allowed of FA and the highest value of nS. The results were compared with real experimental values when available for the validation purposes, obtaining a difference within 1%. The percentage of loss of compressive strength raised as the proportion of fly ash in the mixture increased. If we replaced PC with a combination of 20% FA and 6% nS (resulting in a total of 26%), the subsequent loss of compressive strength would be 10.8%. However, if we replaced PC with a combination of 40% of FA and 6% of nS (resulting in a total of 46%), the subsequent loss of compressive strength would be 26.3%.

If we allow the optimization procedure to select a solution between the original component constraints, the use of fly ash is not necessary in the mixture in order to maximize the compressive strength (Table 2.15). Figure 2.13 shows that when the model is forced to include FA in the mixture, the user has to be willing to lose compressive strength although at a lower rate than that described by a linear loss. When a lower bound is set for FA, the optimizer keeps nS fixed at its highest level, while varying the PC fraction. This indicates that there is a greater loss of compressive strength by reducing nS than by reducing PC.

Table 2.16 presents an additional analysis, this time varying the nS proportion in the mixture controlled by its upper bound. The optimizer kept the quantity of nS at the highest value allowed to gain more compressive strength. Such gain became approximately linear when keeping FA at its lowest level (zero in this case). Figure 2.14 shows the increment in compressive strength with respect to the nS proportion. According to this figure, for example, when adding 3% of nS the compressive strength would increase 8.9%; adding 6%, the compressive strength rises 14.1% in the absence of fly ash (Table 2.16).

Table 2.16 Optimization results varying of the upper constraint of nS.

Variation of Nano-Silica	ε=	**0**	**0.01**	**0.02**	**0.03**	**0.04**	**0.05**	**0.06**
Optimizer Value (MPa)	Z=	**63.20**	**65.33**	**67.20**	**68.82**	**70.17**	**71.26**	**72.09**
Experimental Value (MPa)	Z=	**64.01**	**-**	**-**	**66.99**	**-**	**-**	**73.15**
Decision Variables in Proportions	PC=	1.00	0.99	0.98	0.97	0.96	0.95	0.94
	FA=	0.00	0.00	0.00	0.00	0.00	0.00	0.00
	nS=	0.00	0.01	0.02	0.03	0.04	0.05	0.06
	w/b=	0.3	0.3	0.3	0.3	0.3	0.3	0.3
Percentage of gain of Compressive Strength		-	3.4%	6.3%	8.9%	11.0%	12.7%	14.1%

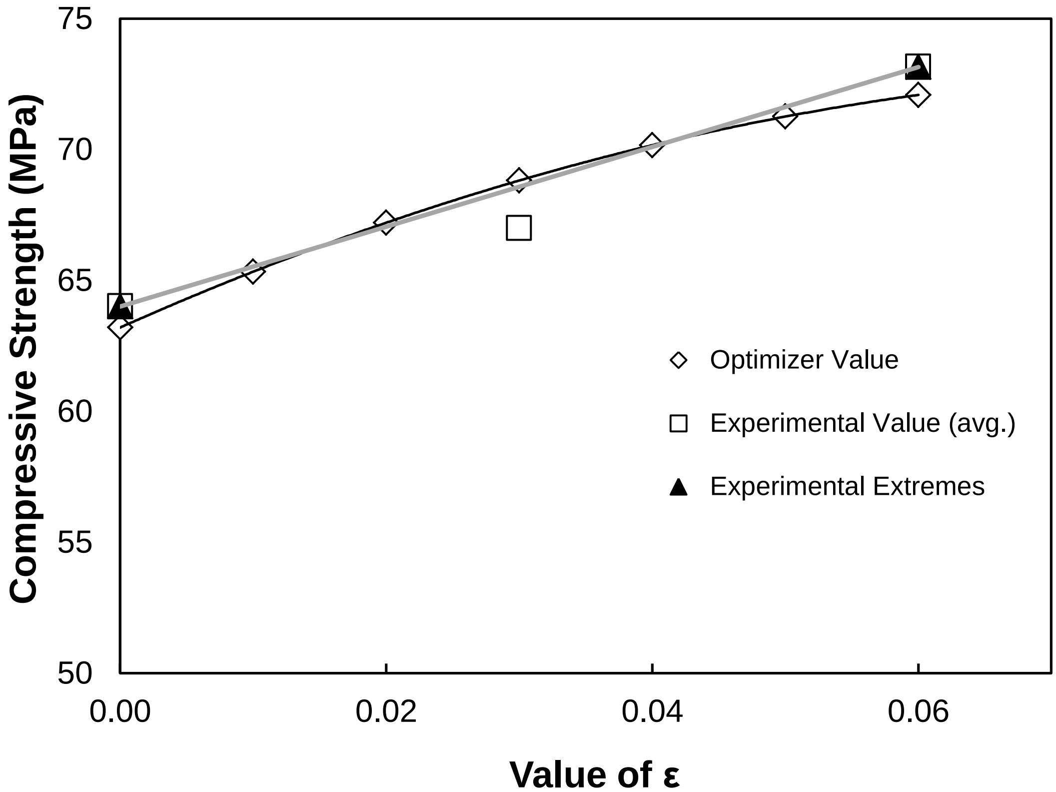

Figure 2.14 Variation in concrete compressive strength as nS increases (FA set at 0.0).

In the proceeding analysis the value of nS was set to 0% in the optimization model while we varied the FA lower bound to compare the results with the previous analyses. Figure 2.15 shows the difference between replacing cement with just FA and replacing cement with both FA and nS. One can observe that as cement is replaced, the percentage of difference in compressive strength between adding or not adding nS increases (Table 2.17). For example, based on the evaluated experimental conditions, if cement is replaced in a concrete mixture with 40% of FA, the expected compressive strength in day 7 will be 33.03 MPa; then, if cement is replaced with 40% of FA with an additional 6% of nS, the expected compressive strength in day 7 will be 53.10 MPa. Therefore, if nS is added there would be a 60.8% difference in compressive strength at day 7.

Table 2.17 Comparison between optimizer results of mixtures with and without nS.

Variation of Fly Ash	ε=	**0**	**0.10**	**0.20**	**0.30**	**0.40**
Optimizer Value with nS=0.06 (MPa)	Z_{nS}=	**72.09**	**68.63**	**64.31**	**59.14**	**53.10**
Optimizer Value with nS=0.0 (MPa)	Z_{wnS} =	**63.20**	**56.75**	**49.57**	**41.66**	**33.03**
Difference (MPa)	-	8.89	11.88	14.74	17.47	20.07
Percentage of Difference	-	14.1%	20.9%	29.7%	41.9%	60.8%

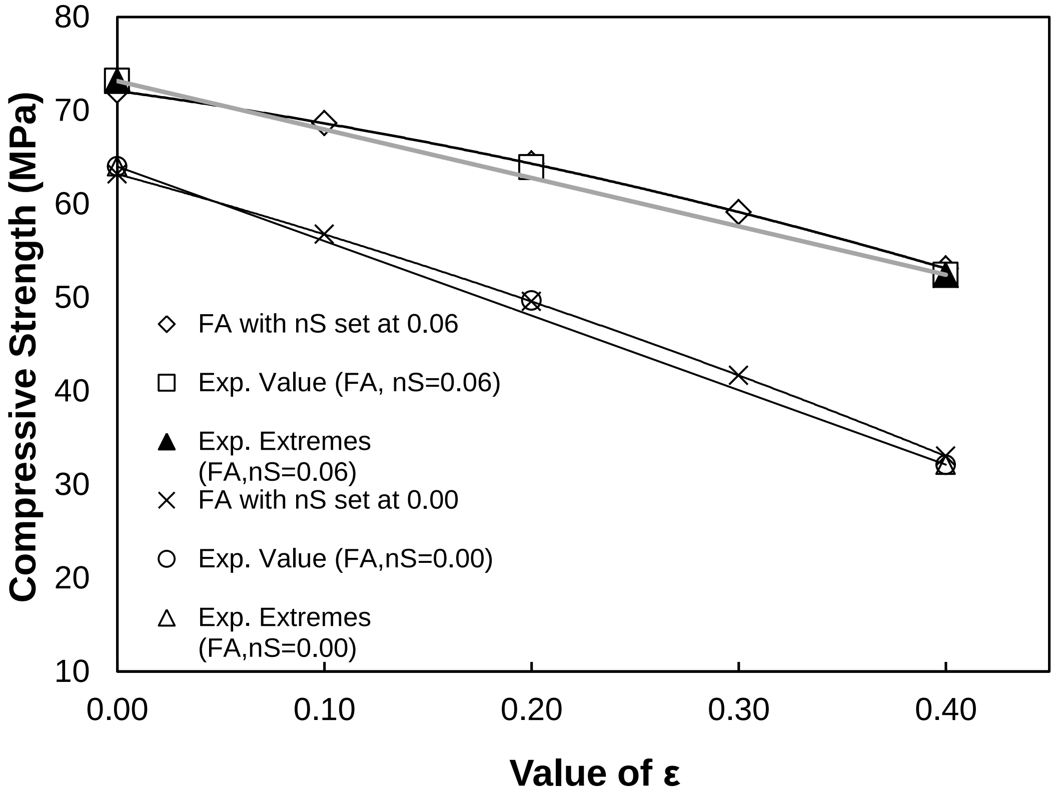

Figure 2.15 Comparison graph between mixtures containing FA with and without nS.

As mentioned, three replicates were considered in this experiment following ASTM C192/C192M − 13a [51]. Such sample size, when analyzed statistically through the use of an operating characteristic curve, is capable of detecting differences in compressive strength larger than 8 MPa. A difference of 8 MPa can be correctly detected with a probability of 78.5%. Because the minimum difference between mixtures with and without nS in our experiment was 8.89 MPa (Table 2.17), the chosen number of replicates was deemed adequate for analysis.

2.7. Final Remarks

A design of experiments with mixtures was proposed and carried out here to characterize compressive properties in time as a function of the proportions of Portland cement, fly ash, nanosilica, and the water-to-binder ratio. This experiment allowed obtaining regression models that were subsequently used to set up a series of optimization problems to maximize the compressive strength of the mixture.

The addition of fly ash to concrete, as shown in this experiment, caused a loss of compressive strength at early age. Thus, to offset such loss, the addition of nanosilica is deemed as a plausible alternative. The results provided in this study serve as a guide to control these additions in order to design a material that withstands a desired level of compressive strength.

Instead of one performance measures evaluated here, in the next chapter three performance measures are going to be considered. These are concrete bulk density, percentage of voids, and compressive strength. The analysis will allow identifying the best compromise mixtures in terms of the mentioned criteria.

III. CHAPTER

3. Multiple Criteria Optimization for Cement Mixtures Containing Mineral Admixtures

3.1. Introduction

Recently the construction industry has been forced to seek for alternatives that reduce the environmental damages of producing construction materials [29]. As mentioned, one alternative is to replace cement by FA while the use of nS combined with FA is highly recommended. These nanoparticles improve some valuable concrete properties such as the compressive strength, density, and low porosity [14], [25]. Of them the concrete compressive strength is the mechanical property most relevant and, therefore, the most studied [55]. High values of compressive strength are desired since sometimes the structures should tolerate big loads. The porosity of concrete is related with its durability and permeability [20], [56]. Those characteristic depend of the number, size, and distribution of pores in the cement paste and the aggregates [57]. Thus, the percentage of voids, as a measurement of porosity, is preferred to be lower in concrete structures. On the other hand, concrete with high density values is necessary for shielding against hazardous materials and other applications [58]. Also a high density concrete can represent smaller total concrete volumes required.

Different values of the mechanical and physical properties of concrete are preferred when mineral admixtures are utilized [21], [59]. Also, the desired characteristics depends of the proposed application. In previous works we could note that the specimen with higher compression strength not necessarily corresponds to the ones with higher density and lower porosity [11], [19]. That is why, in some cases, designers have to prioritize, for example, increasing one characteristic and decreasing other ones.

Specifically, this work will focus on the concrete bulk density, percentage of voids, and compressive strength in order to design a multifunctional structural material. This study is paramount since the specimens with higher compressive strength are not necessarily the ones with higher density and lower porosity, that are usually desirable properties in concrete structures [11], [19]. Therefore, there exists a conflict among the different performance measures. For that reason, a multiple criteria optimization was utilized to simultaneously maximize compressive strength and density and to minimize the material porosity. Additional experiments were developed to obtain the previous mentioned performance measures. Finally, the use of this approach helps to identify the mixtures that belong to the Pareto efficient frontier [39], [40]. These mixtures were the best compromise among all performance measures between the set of mixtures under evaluation. The proportions and characteristics of the recommended mixtures are presented and discussed as part of this work.

3.2. Background

3.2.1. Multiple Criteria Optimization

According to Ehrgott the solution of a decision problem is to choose the best alternatives among a set of solutions, where some criteria measure the quality of the alternatives [60]. Nowadays, a variety of optimization methods permit to resolve decision problems that just consider one objective or performance measures. Some of these methods are the simplex method, gradient, and evolutionary optimization.

However, the majority of the engineering decision problems are based on multiple criteria. Therefore, the utilization of multiple criteria optimization have become popular and useful; since this methodology consists of simultaneously optimizing several objectives [18], [61]. Nevertheless, there is a problem when the objectives are in conflict. This means that the optimal solution in an objective is not the same than in other objective.

The objective when solving a multiple criteria optimization problem is to find a set of efficient solutions. These are also known as “Pareto-optimal solutions” or “Pareto-efficient solutions” [36], [39], [61]. These solutions are the best compromise among all performance measures under evaluation; they are deemed equally efficient since a gain in one objective will result in a sacrifice in at least another objective. The efficient solutions form the Pareto efficient frontier.

In order to identify the optimal solutions, we will utilize the Pareto-optimality conditions as described in Deb’s work [61]:

“A solution $x^{(1)}$ is said to dominate the other solution $x^{(2)}$, if both the following conditions are true:

1. The solution $x^{(1)}$ is no worse than $x^{(2)}$ in all objectives. Thus, the solutions are compared based on their objective function values (or location of the corresponding points ($z^{(1)}$ and $z^{(2)}$) on the objective space).
2. The solution $x^{(1)}$ is strictly better than $x^{(2)}$ in at least one objective. ”

Figure 3.1 shows a set of nine solutions in which the domination concept can be graphically explained. Here we want to minimize both objectives (f_1 and f_2). A comparison between two solution points can be made utilizing both Pareto conditions; through this means we can know if a solution point is dominated or non-dominated by other solution. In Figure 3.1, the solutions 1, 3, 4, and 6 are the non-dominated set (the line that joins them is just for representation and not necessary the shape of the efficient frontier).

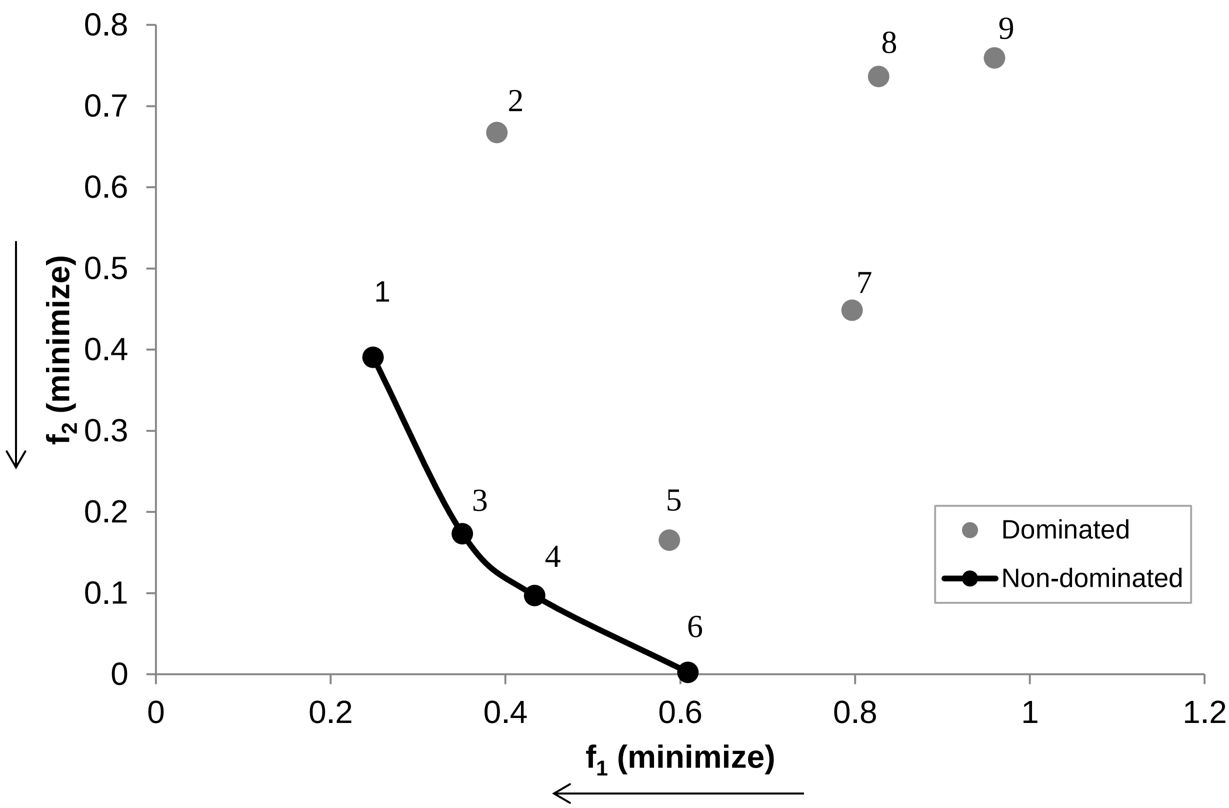

Figure 3.1 Illustration of non-dominated solution points.

The cone of dominance define sets of nonnegative elements in the real space of n dimensions [60]. In addition, the cone of dominance can be used to determine whether a solution point is dominated or non-dominated among the set of solutions under evaluation [60]. This is by applying to each solution point an arrow with the direction of each objective function. In our example, we are minimizing both objectives and, for that reason, the arrows should be used as shown in Figure 3.2. If we apply the cone of dominance to a solution point and the cone is empty, this means that that point is non-dominated [60]. On the other hand, if the cone contains other points that solution point is dominated by the points contained in the cone. For example, if we apply the cone of dominance to the point number 7 we can observe that the cone is not empty. Therefore, there are solutions better that that point such as point 1, 3, 4, 5 and 6. However if we apply the cone of dominance to point number 1, we can notice that the cone is empty. This means that point number 1 is non-dominated by any other member of the solution set. All the non-dominated points constitute a front when they are viewed on the criterion space; together they are also known as the Pareto efficient frontier [61].

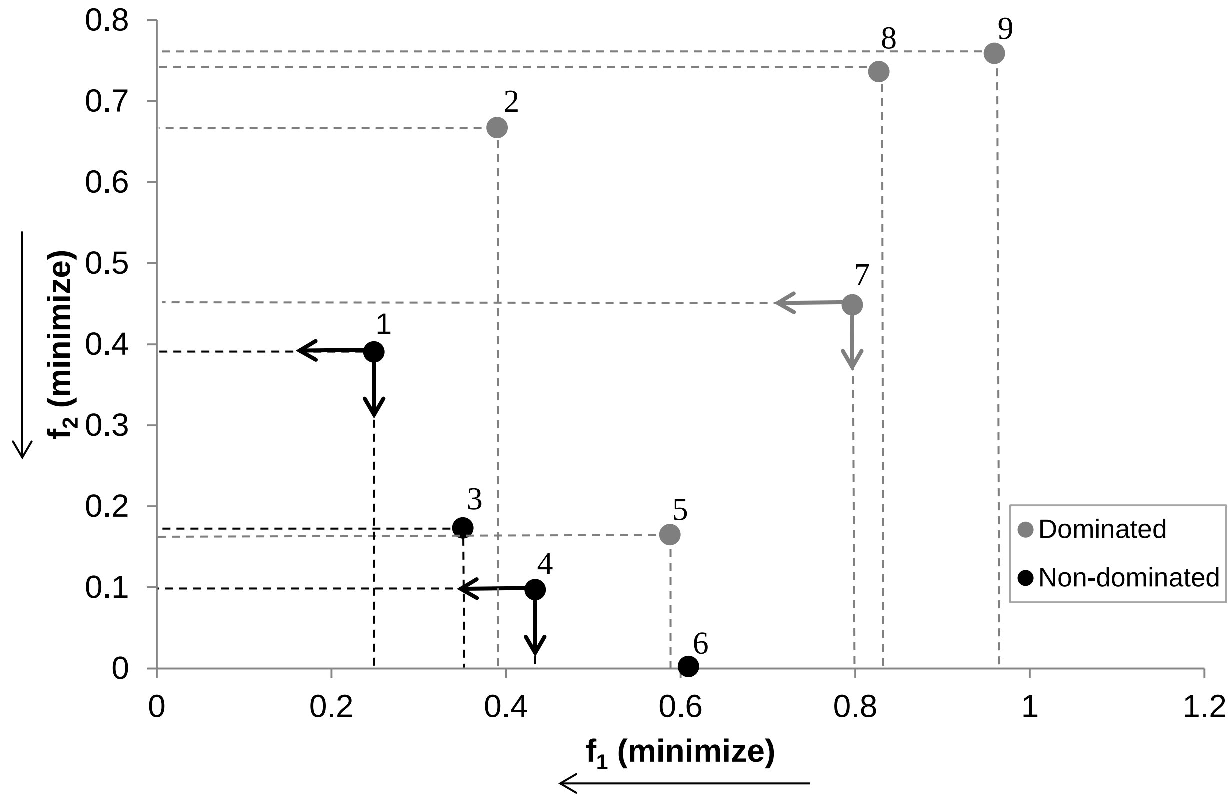

Figure 3.2 Illustration of the cone of dominance.

The cone of dominance can also be applied in optimization problems with three objectives [39]. However, when there are more than three objectives in a multiple criteria optimization problem the visualization of the cone is out of reach.

After finding the Pareto efficient frontier, we cannot select all the efficient solutions in real applications. A single selection has to be made among the set of efficient solutions. Hence, as decision maker, one has to take the final decision among the "optimal solutions" that the multiple criteria optimization provides.

In order to solve the multiple criteria optimization problems to optimality, researchers have developed some methods that are exact and others methods that are heuristics [30], [39], [40], [61]. An exact multiple criteria optimization method found all the solutions that belong to the Pareto efficient frontier. Some of these recent methods consider the Karush-Kuhn-Tucker (KKT) conditions to resolve this kind of problems to optimality [60], [61]. On the other hand, the heuristics multiple criteria optimization methods found solution points that are close to the Pareto efficient frontier; also these methods utilize qualitative considerations to finally recommend a single efficient solution [61].

In a multiple criteria optimization problem the objectives functions can be either maximized or minimized. According to Deb [61], the general form of a multiple criteria optimization problem is as follows:

$$
\begin{array}{lll}
\text{Minimize/Maximize} & f_m(x), & m = 1, 2, \dots, M; \\
\text{Subject to} & g_j(x) \geq 0, & j = 1, 2, \dots, J; \\
 & h_k(x) = 0, & k = 1, 2, \dots, K; \\
 & x_i^{(L)} \leq x_i \leq x_i^{(U)}, & i = 1, 2, \dots, n;
\end{array}
$$

where x_i represents a decision variable from a set of size n. The decision space is the feasible set of the decision variables. On the other hand, the criterion space is formed by all functions.

3.3. Methodology

3.3.1. Multiple Criteria Optimization for Cement Mixtures

A design of experiment for mixtures was utilized in order to generate the different combinations of the cement mixture components, i.e. PC, FA, and nS [4], [8]. For this second stage, the upper bound of nS was changed to 3%. This is because the nanoparticles were diluted in water (50% water and 50% nS) and this fact was not considered properly when changing the proportions to grams. In addition, only the mixtures with water to binder of 0.3 were considered. This decision was taken since those mixtures had higher compressive strength than mixtures with water to binder of 0.5.

Nine component combinations or mixtures were evaluated (Table 3.1). Each one of these mixtures represent a solution k for us since they have different characteristics in terms of physical and mechanical properties of the resulted concrete. Multiple criteria optimization helps us in the decision making process of recommend some of these mixtures.

Table 3.1 Mixture proportion combinations evaluated

k	**Portland Cement**	**Fly Ash**	**nano-Silica**
1	0.800	0.200	0.000
2	1.000	0.000	0.000
3	0.600	0.400	0.000
4	0.585	0.400	0.015
5	0.770	0.200	0.030
6	0.985	0.000	0.015
7	0.970	0.000	0.030
8	0.785	0.200	0.015
9	0.570	0.400	0.030

Now we should present our problem as a multiple criteria optimization problem. We are interested in recommending an alternative (k*) among the different mixture proportions of PC, FA, and nS that we generated (Table 3.1). The decision taken will be based in terms our performance measures, i.e. compressive strength, bulk density, and percentage of voids of the resulted specimens (Figure 3.3). In this work, the desired properties are higher compressive strength and density and lower percentage of voids.

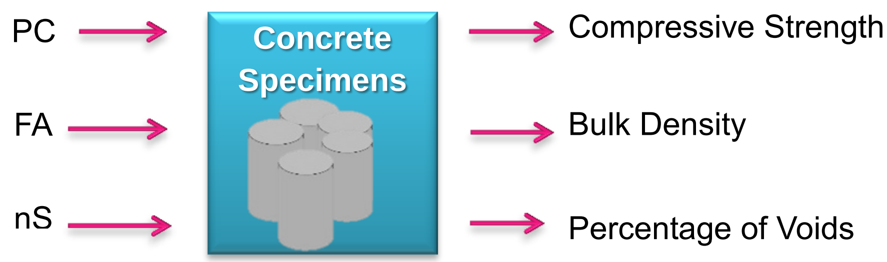

Figure 3.3 System diagram with the input and output variables.

Consider the following multiple criteria optimization problem:

Find PC, FA, and nS in order to:

Maximize $f_1(\mathbf{x})$, $f_2(\mathbf{x})$

Minimize $f_3(\mathbf{x})$

Subject to:

$$0.57 \leq PC \leq 1.00$$

$$0.00 \leq FA \leq 0.40$$

$$0.00 \leq nS \leq 0.03$$

where $f_1(\mathbf{x})$ is the compressive strength, $f_2(\mathbf{x})$ is the bulk density, and $f_3(\mathbf{x})$ is the percentage of voids of the respective specimens.

We intent to restrict the problem described above to a manageable number of sampling experimental solutions generated through a mixture DOE. Furthermore, the best tradeoffs among the competing criteria were identified with the application of Pareto-optimality conditions as advocated by the Applied Optimization Group in [39]–[41].

The method employed to resolve the multiple criteria optimization problem is an exact method based on the Pareto-optimality conditions when having a finite number of solutions [39], [40]. This method has being utilized to solve engineering and science problems by the Applied Optimization Group. Specifically, it was utilized to analyze process windows for injection molding considering two and three performance measures [40]. In addition, this method had been used to find potential biomarkers of lung cancer [39]. This time the method was used to effectively find the proportion combinations of a cement mixture that belong to the Pareto-efficient frontier.

The method was coded in Microsoft Excel ® for the availability of the program. As the tool is coded to minimize all the performance measures, the following transformation was necessary to change from maximization to minimization in the case of compressive strength and bulk density [41]:

$$f_{i0}^{*} = (Max\ f_{i0} + Min\ f_{i0}) - f_{i0}$$

Equation 1

where i is varying from 1 to k solutions and *j* is set to the particular criterion 0.

Utilizing the Pareto-optimality conditions, as aforementioned, a full pairwise comparison was performed between the solutions to eventually find the Pareto-efficient frontier or the non-dominated set. A detailed description of the multiple criteria optimization method utilized in this work can be found in Camacho's work [62].

3.3.2. Experimental Conditions

For this second stage some changes were necessary in preparing the mixtures. Via a granulometry study, the experimental proportions of the aggregates were determined as: 30% of gravel, 35% of processed-aggregate, and 35% of clean river sand. The same characteristics of the mixtures were taken into account, i.e. segregation, bleeding, slump loss, and consistency, in order to determine the quantity of polycarboxylate superplasticizer (SP) necessary for each mixture.

3.3.3. Materials

The materials utilized in this stage are described in this section since they have different properties than the listed before. This is because they become from different lots and suppliers. However, these materials were the same during the second phase of the experiment.

Aggregates

Gravel was used as coarse aggregate and its maximum diameter was 19.0 mm. Moreover, the processed-aggregate had a maximum diameter of 9.5 mm. The fineness modulus of the fine aggregate, i.e. beach sand, was 3.0.

Table 3.2 Properties of the aggregates.

Aggregate	Apparent Specific Gravity	Specific Gravity (Oven-dry)	Specific Gravity (SSD)	Absorption (%)	Unit Weight (kg/m^3)
Gravel	2.88	2.71	2.77	2.09	1584.70
Processed-aggregate	2.77	2.50	2.59	3.86	1740.57
Beach Sand	2.65	2.42	2.51	3.48	1460.54

Portland Cement

The PC Type I utilized to prepare the mixtures had a specific gravity of 3.06.

Fly Ash

The FA class F used for the mixtures possessed a specific gravity of 2.38.

Nanosilica

The nS used in this second stage was obtained from Nissan Chemical Industries and originally suspended in an aqueous solution, with a particles mean size of 69.40 nm and specific gravity of 2.03 (Figure 3.5). As a note, these nanoparticles are three times bigger than the used in the first stage (23.22 nm).

Superplasticizer

The polycarboxylate superplasticizer used was the ADVA 575 and was obtained from Instron in PR.

Water

The water used to prepare the mixtures was tap water at room temperature.

3.3.4. Fabrication and Testing Procedure

A Globe mixer machine was utilized to mix the concrete components (Figure 3.4). The coarse and fine aggregates were first dry-mixed and then introduced into the mixer for 0.25 min at 120 rpm, followed by the addition of half of the required water. Then the PC was added to the mixer followed by the amount of FA (when necessary) for 0.25 min at 60 rpm. The nS and SP were diluted in water in order to obtain a uniform distribution of the particles throughout the mixture and added to the mixer (when used) for 4.30 min at 120 rpm.

The concrete cylinders prepared were filled by the rodding method [51]. The cylinders were demolded and placed in limewater until tested at normal curing conditions (20-23ºC and RH=100%). The temperature (23-25ºC) in the experiment was relatively constant.

The standard procedure [63] was followed to measure the density and the percentage of voids of the specimens. In order to meet the minimum volume required by the standard [52], the dimensions of the test cylinders were 76 mm in diameter and 152 mm in length (Figure 3.6). On the other hand for the compressive strength test, the dimensions of the test cylinders were 50 mm in diameter and 100 mm in length (Figure 3.6) [52].

Figure 3.4 Globe mixer machine utilized.

Figure 3.5 Example of the silica nanoparticles utilized as dust.

Figure 3.6 Example of concrete cylinders prepared (76 by 152 mm & 50 by 100 mm).

Six cylinders were tested for compressive strength at 7, 28, and 90 days of curing. The compression tests were performed in a 3000 kN Forney universal test machine according to ASTM C39/C39M-12a [53].

Moreover, ASTM C642-13 was followed to measure the density and percentage of voids of five specimens [63]. The test was at 7, 28, and 90 days. In this test the specimen oven-dry mass (A), saturated mass after immersion in water (B), saturated mass after boiling (C), and immersed apparent mass (D) were considered. These values were used to calculate the bulk density, apparent density, and the volume of permeable pore space or percentage of voids of the specimens.

3.4. Results

All the specimens generated were tested for compressive strength, bulk density, and percentage of voids at 7, 28, and 90 days of curing. However, since the work scope is until age 28 the results presented in this section will be for 7 and 28 days only. The results of 90 days will be used in a future work.

3.4.5. Results from day 7

First, the summary of results obtained in day 7 are presented in Table 3.3. The average of the compressive strength results is from 6 replicates whereas for the bulk density and percentage of voids the average results is from 5 replicates. In addition, the variability between the replicates for each performance measures can be showed in the following boxplots: Figure 3.8, Figure 3.9, and Figure 3.10. If we consider each one of the performance measures separately, they will aim at different solutions (Figure 3.7). In other words the performance measures are in conflict. Now, each one of the mixtures combination will represent a solution or alternative (k) for our multiple criteria optimization problem (Table 3.3).

Table 3.3 Average result of performance measures at day 7.

k	Mixture Proportions (PC/FA/nS)	Compressive Strength		Bulk Density		Volume of Permeable Pore Space	
		Average	Std. Dev.	Average	Std. Dev.	Average	Std. Dev.
		MPa	MPa	Kg/m^3	Kg/m^3	%	%
1	0.800/0.20/0.000	27.37	1.15	2165.88	37.32	15.59	0.98
2	1.000/0.00/0.000	31.11	7.22	2218.43	34.71	13.85	0.75
3	0.600/0.40/0.000	33.71	3.19	2117.88	13.27	17.42	0.32
4	0.585/0.40/0.015	31.58	5.32	2125.56	29.80	16.58	0.70
5	0.770/0.20/0.030	29.75	5.24	2186.46	16.19	15.93	0.63
6	0.985/0.00/0.015	27.03	5.65	2188.51	37.78	16.00	1.05
7	0.970/0.00/0.030	24.19	8.24	2189.98	14.19	16.04	0.31
8	0.785/0.20/0.015	40.40	2.47	2156.64	6.26	17.00	0.28
9	0.570/0.40/0.030	33.35	4.63	2163.49	23.10	12.49	0.78

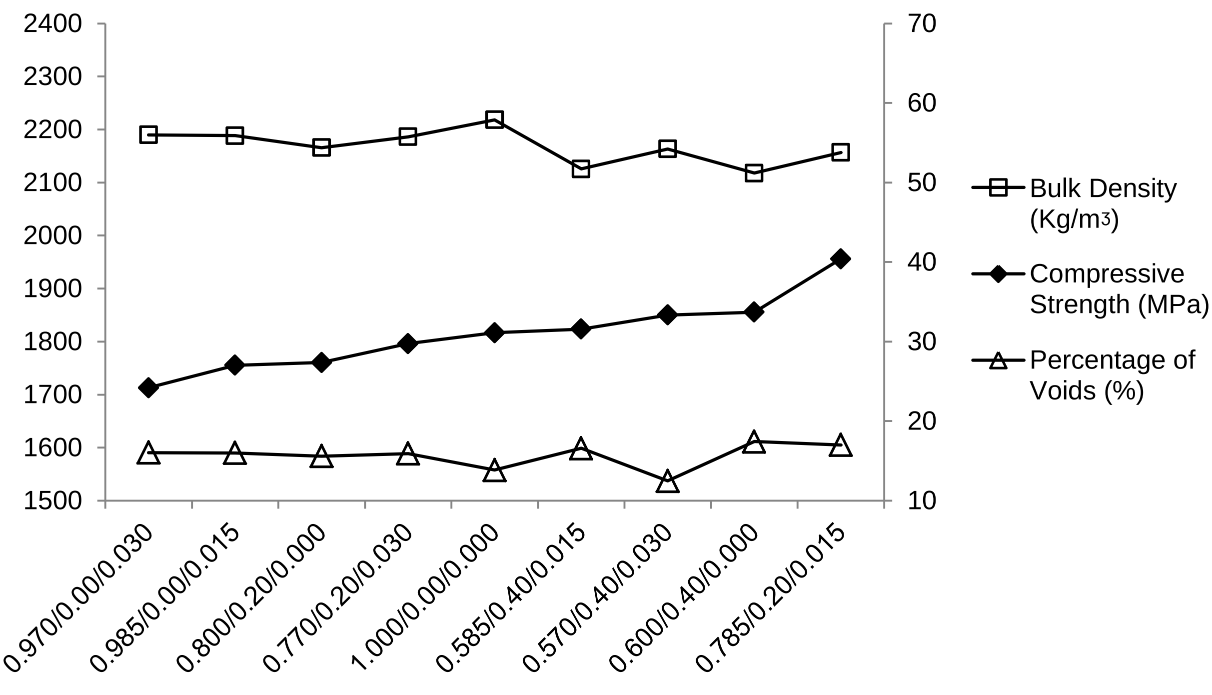

Figure 3.7 Average result from the performance measures at day 7.

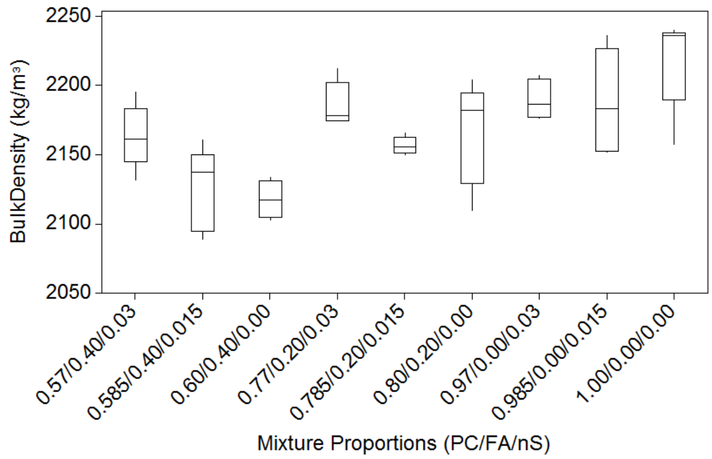

Figure 3.8 Boxplots of mixtures bulk density at 7 days.

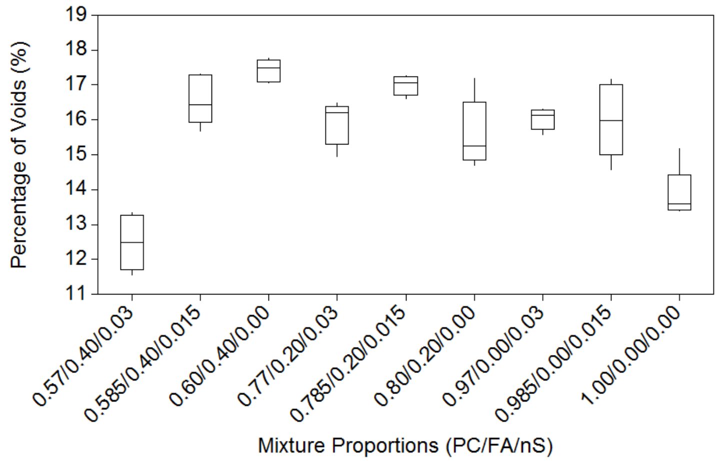

Figure 3.9 Boxplots of mixtures percentage of voids at 7 days.

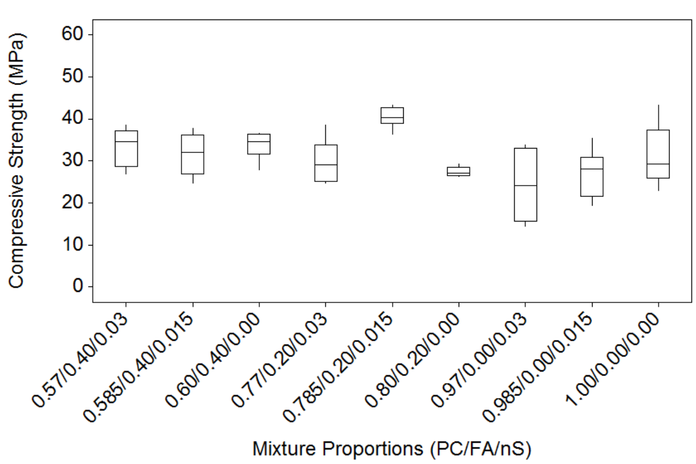

Figure 3.10 Boxplots of mixtures' compressive strength at 7 days.

Compressive strength, bulk density, and percentage of voids were represented as f_1, f_2, and f_3 respectively. Then the values of our performance measures, i.e. f_1, f_2, and f_3, were utilized to create three matrices A_1, A_2, and A_3 to compare all the solutions *n* in each objective.

Table 3.44 shows in bold the efficient solutions from day 7; these are mixture number 2, 8, and 9. Mixture number 2 is the control mixture with just PC. It was expected that this mixture was in the optimal set since its properties are very appropriate during its early age. However, it is very interesting that the other two mixtures (8 and 9) that belong to the Pareto-efficient frontier contains FA and nS. These mixtures are mixture number 8 that have 78.5% of PC, 20% of FA, and 1.5% nS; and mixture number 9 that have 57% of PC, 40% of FA, and 3% nS. Although mixture number 9 have 40% of FA (high level of replacement), the addition of 3% of nS makes it a competitive combination with adequate physical and mechanical concrete properties. In contrast, mixture number 3 have 60% of PC, 40% of FA, and 0% nS (high level of replacement) but it does not belong to the Pareto-efficient frontier. The same case is for mixture number 1 with 20% of FA and 0% of nS. The difference between being part or not of the Pareto-efficient frontier appears to be the addition of silica nanoparticles.

Table 3.4 Mixtures highlighted belong to the Pareto efficient frontier of day 7.

k	Mixture Proportions (PC/FA/nS)	f_1	f_2	f_3
		MPa	Kg/m^3	%
1	0.800/0.20/0.000	27.37	2165.88	15.59
2	**1.000/0.00/0.000**	**31.11**	**2218.43**	**13.85**
3	0.600/0.40/0.000	33.71	2117.88	17.42
4	0.585/0.40/0.015	31.58	2125.56	16.58
5	0.770/0.20/0.030	29.75	2186.46	15.93
6	0.985/0.00/0.015	27.03	2188.51	16.00
7	0.970/0.00/0.030	24.19	2189.98	16.04
8	**0.785/0.20/0.015**	**40.40**	**2156.64**	**17.00**
9	**0.570/0.40/0.030**	**33.35**	**2163.49**	**12.49**

As we are considering three performance measures, the results can still be presented in a 3D graph. In addition, the cone of dominance can be utilized to visualize the dominated and non-dominated solutions. Figure 3.11 shows all the solutions k (mixtures) in the criterion space with a rotated view to make easier the visualization of the efficient frontier.

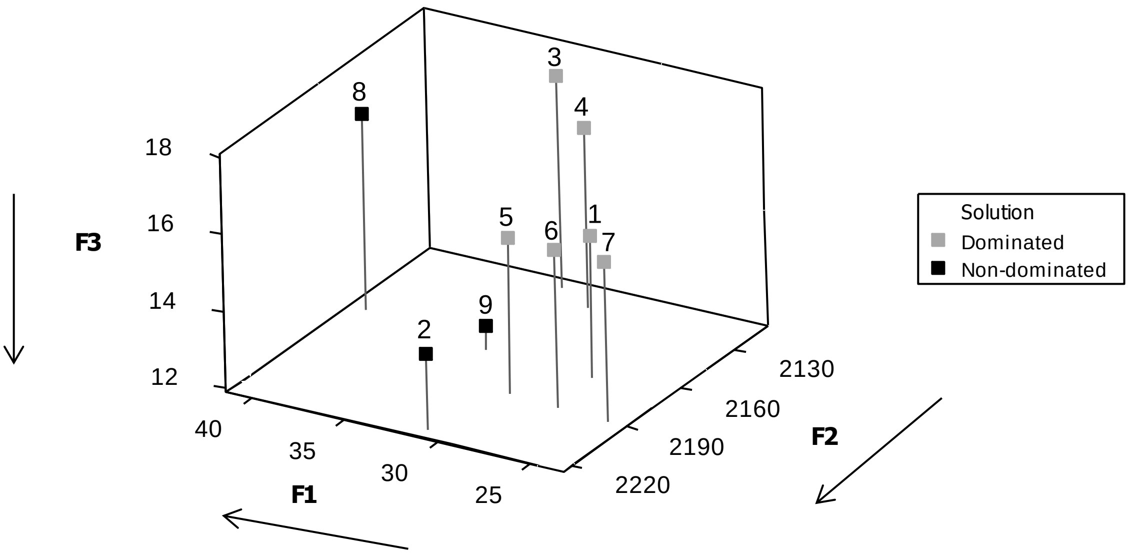

Figure 3.11 Graphical results of the solution set evaluated at 7 days (rotated view).

Figure 3.12 shows an example of a dominated solution. This time, the cone of dominance is applied to the solution evaluated (mixture number 1) with the arrows pointing to the preference direction of each axis. As we can observe, the cone is not empty, for that reason this solution is dominated. Also this means that that solution is dominated by the solutions contained by the cone. On the other hand, Figure 3.13 shows an example of a non-dominated solution. The cone of dominance of solution number 8 is empty; therefore, it is non-dominated by any other solution in the solution set evaluated. This solution, in conjunction with the other non-dominated solutions, form the Pareto-efficient frontier. Figure 3.14 show all the solutions in the criterion space but this time with the common axis orientation.

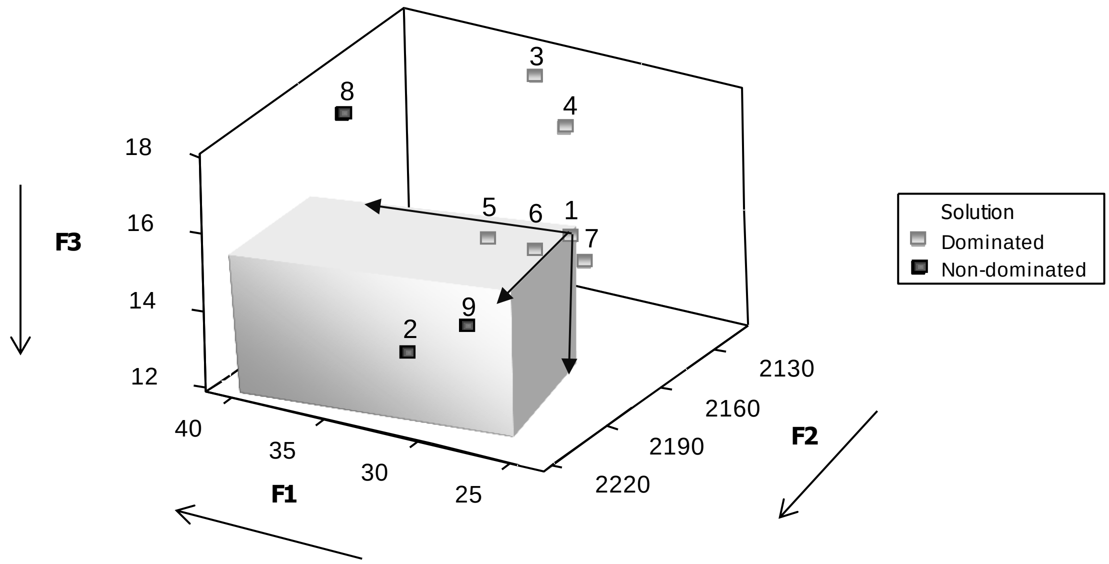

Figure 3.12 Cone of dominance applied to a dominated solution.

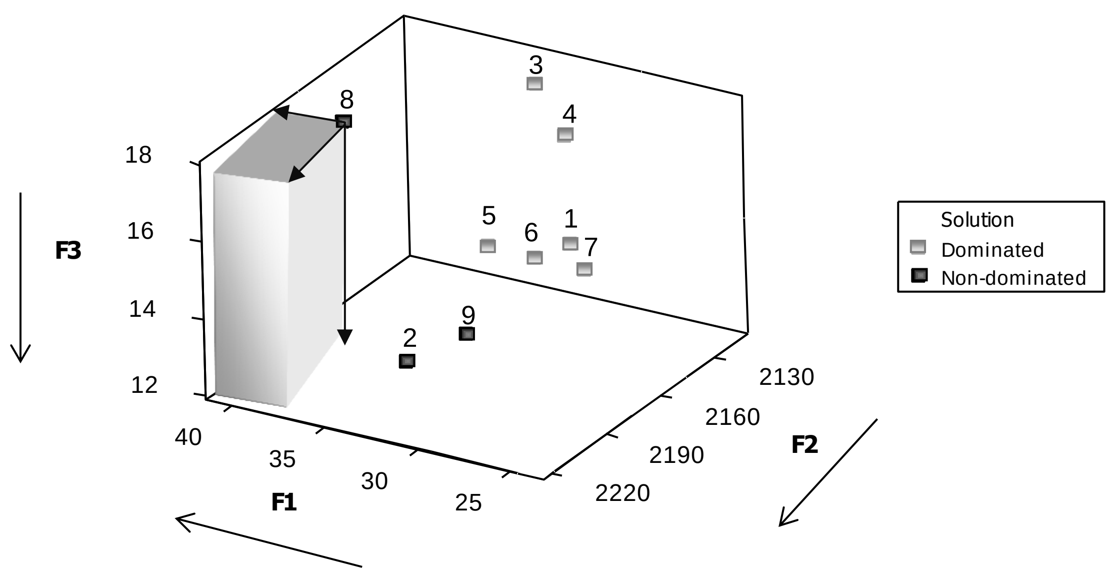

Figure 3.13 Cone of dominance applied to a non-dominated solution.

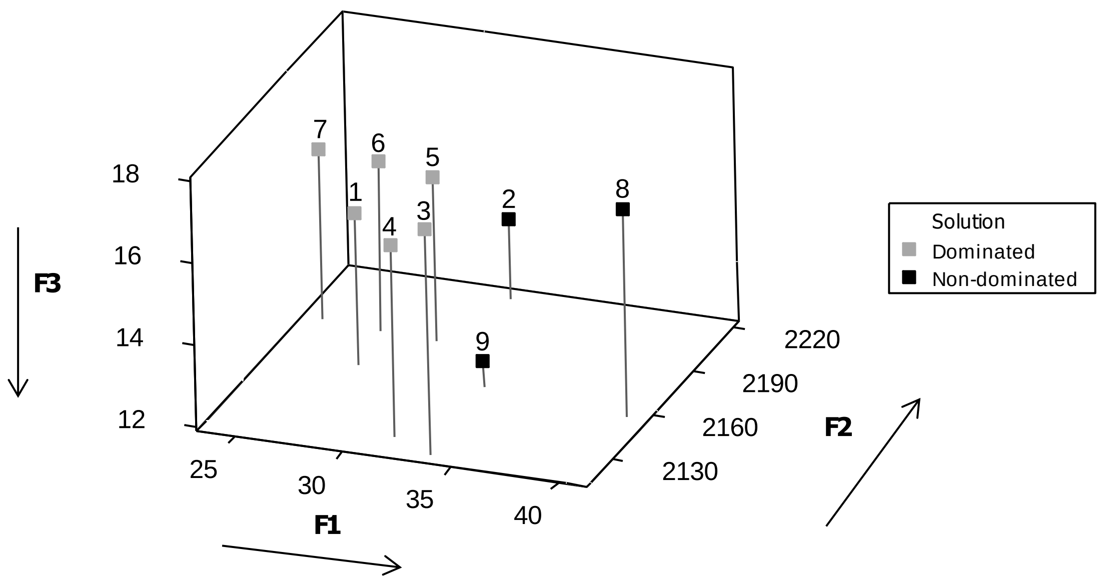

Figure 3.14 Graphical results of the solution set evaluated at 7 days.

3.4.6. Results from day 28

Table 3.5 and Figure 3.15 show the average results of the three performance measures evaluated. In addition, the variability of each mixture is presented in the boxplots of compressive strength, bulk density, and percentage of voids (Figure 3.16, Figure 3.17, and Figure 3.18). Here we can observe that mixture number 8 has a higher value of compressive strength. However, mixture number 6 has the higher value of bulk density and the lower percentage of voids (Figure 3.15). There still exists a conflict between the objectives.

Table 3.5 Average result of performance measures at day 28.

k	Mixture Proportions (PC/FA/nS)	Compressive Strength		Bulk Density		Volume of Permeable Pore Space	
		Average	Std. Dev.	Average	Std. Dev.	Average	Std. Dev.
		MPa	MPa	Kg/m^3	Kg/m^3	%	%
1	0.800/0.20/0.000	34.48	5.49	2141.12	52.85	15.77	1.20
2	1.000/0.00/0.000	41.91	9.59	2192.05	42.05	14.75	1.06
3	0.600/0.40/0.000	44.09	2.94	2098.88	19.94	17.26	0.61
4	0.585/0.40/0.015	38.92	9.38	2096.61	45.25	17.17	1.24
5	0.770/0.20/0.030	36.59	5.79	2168.71	27.31	16.06	0.86
6	0.985/0.00/0.015	31.29	3.41	2226.15	28.65	14.25	0.63
7	0.970/0.00/0.030	31.81	4.64	2197.49	22.35	15.35	0.43
8	0.785/0.20/0.015	47.27	6.58	2179.52	12.47	16.12	0.25
9	0.570/0.40/0.030	41.5	3.23	2131.97	18.65	16.02	0.57

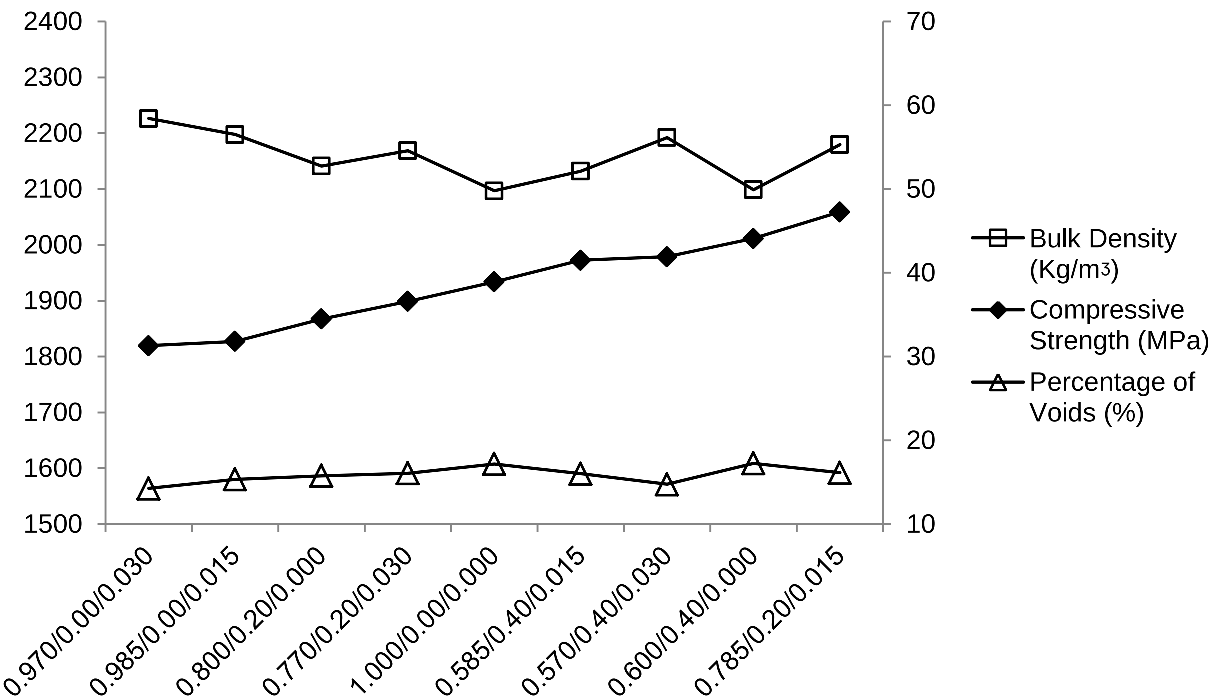

Figure 3.15 Average result from the performance measures at day 28.

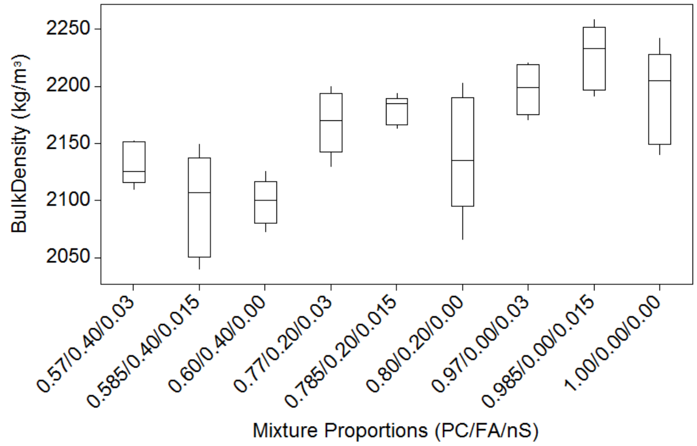

Figure 3.16 Boxplots of mixtures' bulk density at 28 days.

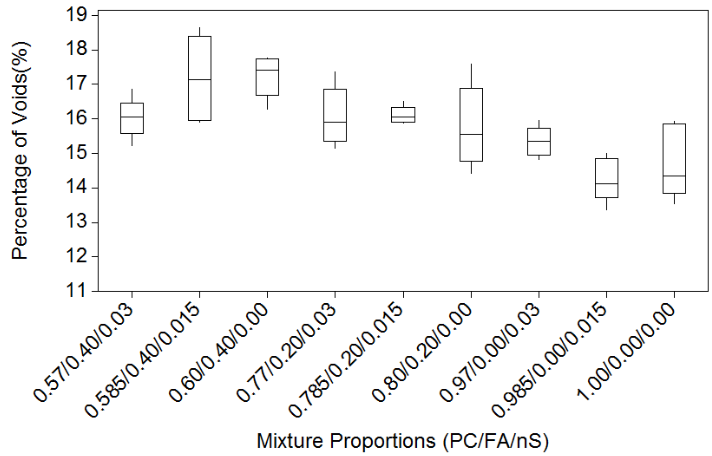

Figure 3.17 Boxplots of mixtures' percentage of voids at 28 days.

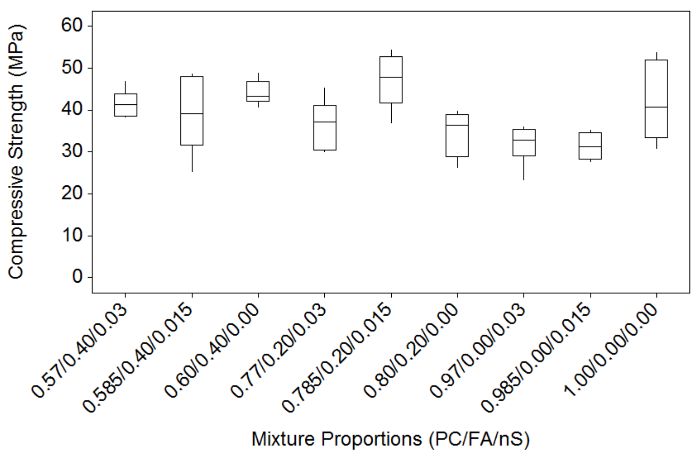

Figure 3.18 Boxplots of mixtures' compressive strength at 28 days.

The aim in this stage is the same as in the analysis of day 7: to maximize compressive strength and bulk density, and to minimize the percentage of voids. The results obtained from the multiple criteria optimization strategy are presented in Table 3.6. This time, there are four solutions that belong to the Pareto efficient frontier. These solutions are mixtures number 2, 6, 7, and 8. The Pareto-optimality conditions can be used to ensure that these sets of mixtures are always better in at least one objective and the same or worse in other objective.

We expected mixture number 2 to be part of the Pareto efficient frontier since it is the control mixture with only PC. Mixtures number 6 and 7 contain PC and 1.5% and 3.0% of nS respectively. These mixtures do not have FA, i.e. the replacement of interest. However, the last mixture that is also efficient contains FA (mixture number 8). This one contains 78.5% of PC, 20% of FA, and 1.5% of nS. The solutions can be observed in the criterion space graphically in Figure 3.19 with a rotated view. However, in Figure 3.20 the solutions are presented with the common axis orientation.

Table 3.6 Mixtures highlighted belong to the Pareto efficient frontier of day 28.

k	Mixture Proportions (PC/FA/nS)	f_1	f_2	f_3
		MPa	Kg/m^3	%
1	0.800/0.20/0.000	34.48	2141.12	15.77
2	**1.000/0.00/0.000**	**41.91**	**2192.05**	**14.75**
3	0.600/0.40/0.000	44.09	2098.88	17.26
4	0.585/0.40/0.015	38.92	2096.61	17.17
5	0.770/0.20/0.030	36.59	2168.71	16.06
6	**0.985/0.00/0.015**	**31.29**	**2226.15**	**14.25**
7	**0.970/0.00/0.030**	**31.81**	**2197.49**	**15.35**
8	**0.785/0.20/0.015**	**47.27**	**2179.52**	**16.12**
9	0.570/0.40/0.030	41.5	2131.97	16.02

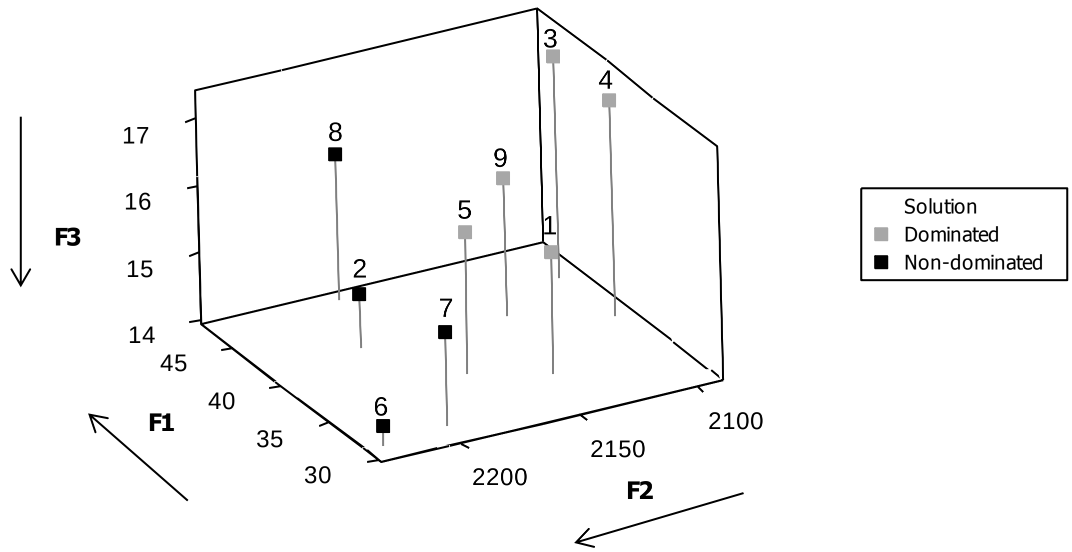

Figure 3.19 Graphical results of the solution set evaluated at 28 days (rotated view).

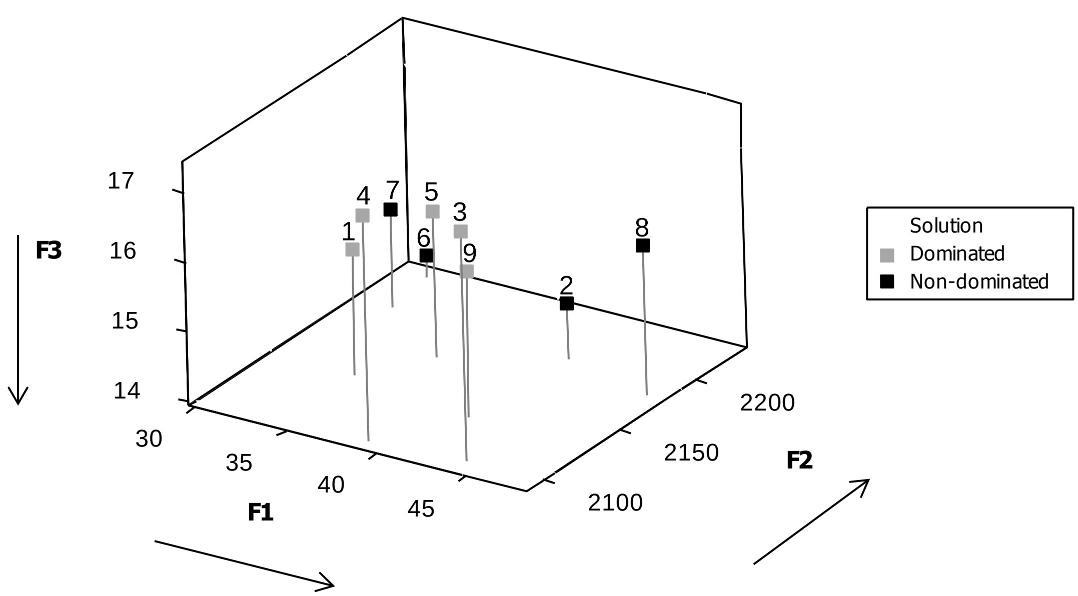

Figure 3.20 Graphical results of the solution set evaluated at 28 days.

3.4.7. Full comparison between the mixtures during all the concrete ages evaluated.

A final analysis was performed on all mixtures, taking into consideration the concrete age or testing day. This full comparison allows us to identify the mixtures that show the better performance in terms of our three performance measures. Table 3.7 presents the eighteen solutions or mixtures with their respective characteristics use for the analysis.

Table 3.7 Data summary from all the mixtures evaluated at all concrete ages.

k	Mixture Proportions (PC/FA/nS)	Testing Day	Compressive Strength		Bulk Density		Volume of Permeable Pore Space	
			Avera-ge	Std. Dev.	Average	Std. Dev.	Average	Std. Dev.
			MPa	MPa	Kg/m^3	Kg/m^3	%	%
1	0.800/0.20/0.000	7	27.37	1.15	2165.88	37.32	15.59	0.98
2	1.000/0.00/0.000	7	31.11	7.22	2218.43	34.71	13.85	0.75
3	0.600/0.40/0.000	7	33.71	3.19	2117.88	13.27	17.42	0.32
4	0.585/0.40/0.015	7	31.58	5.32	2125.56	29.80	16.58	0.70
5	0.770/0.20/0.030	7	29.75	5.24	2186.46	16.19	15.93	0.63
6	0.985/0.00/0.015	7	27.03	5.65	2188.51	37.78	16.00	1.05
7	0.970/0.00/0.030	7	24.19	8.24	2189.98	14.19	16.04	0.31
8	0.785/0.20/0.015	7	40.40	2.47	2156.64	6.26	17.00	0.28
9	0.570/0.40/0.030	7	33.35	4.63	2163.49	23.10	12.49	0.78
10	0.800/0.20/0.000	28	34.48	5.49	2141.12	52.85	15.77	1.20
11	1.000/0.00/0.000	28	41.91	9.59	2192.05	42.05	14.75	1.06
12	0.600/0.40/0.000	28	44.09	2.94	2098.88	19.94	17.26	0.61
13	0.585/0.40/0.015	28	38.92	9.38	2096.61	45.25	17.17	1.24
14	0.770/0.20/0.030	28	36.59	5.79	2168.71	27.31	16.06	0.86
15	0.985/0.00/0.015	28	31.29	3.41	2226.15	28.65	14.25	0.63
16	0.970/0.00/0.030	28	31.81	4.64	2197.49	22.35	15.35	0.43
17	0.785/0.20/0.015	28	47.27	6.58	2179.52	12.47	16.12	0.25
18	0.570/0.40/0.030	28	41.50	3.23	2131.97	18.65	16.02	0.57

The resulting efficient mixtures from this analysis are in bold in Table 3.8. Also the solutions are presented graphically in the Figure 3.21. It is interesting to mention that the control mixture that contains only PC appears in the Pareto efficient frontier with its properties at day 7 and also at day 28. Besides that mixture, all the other mixtures that are part of the Pareto-efficient frontier contain silica nanoparticles. However, there are two mixtures that also have the cement replacement by FA in two levels. These mixtures can be a good option to the users since they contain FA but still possess good mechanical and physical properties. In addition, Figure 3.22 shows the solutions with the common axis orientation.

Table 3.8 Mixtures highlighted belong to the Pareto efficient frontier of the full comparison.

k	Mixture Proportions (PC/FA/nS)	Testing Day	f_1	f_2	f_3
			MPa	Kg/m^3	%
1	0.800/0.20/0.000	7	27.37	2165.88	15.59
2	**1.000/0.00/0.000**	**7**	**31.11**	**2218.43**	**13.85**
3	0.600/0.40/0.000	7	33.71	2117.88	17.42
4	0.585/0.40/0.015	7	31.58	2125.56	16.58
5	0.770/0.20/0.030	7	29.75	2186.46	15.93
6	0.985/0.00/0.015	7	27.03	2188.51	16.00
7	0.970/0.00/0.030	7	24.19	2189.98	16.04
8	0.785/0.20/0.015	7	40.40	2156.64	17.00
9	**0.570/0.40/0.030**	**7**	**33.35**	**2163.49**	**12.49**
10	0.800/0.20/0.000	28	34.48	2141.12	15.77
11	**1.000/0.00/0.000**	**28**	**41.91**	**2192.05**	**14.75**
12	0.600/0.40/0.000	28	44.09	2098.88	17.26
13	0.585/0.40/0.015	28	38.92	2096.61	17.17
14	0.770/0.20/0.030	28	36.59	2168.71	16.06
15	**0.985/0.00/0.015**	**28**	**31.29**	**2226.15**	**14.25**
16	**0.970/0.00/0.030**	**28**	**31.81**	**2197.49**	**15.35**
17	**0.785/0.20/0.015**	**28**	**47.27**	**2179.52**	**16.12**
18	0.570/0.40/0.030	28	41.50	2131.97	16.02

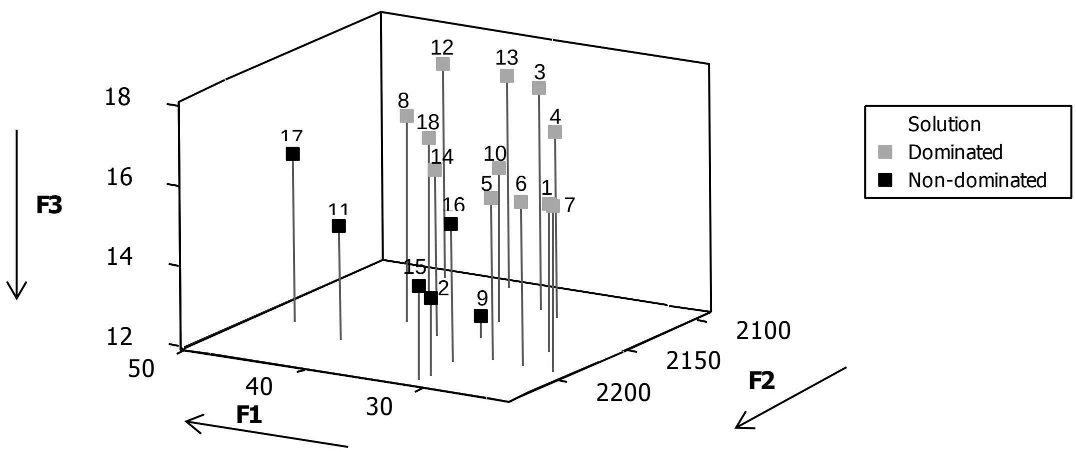

Figure 3.21 Graphical results of the full comparison (rotated view).

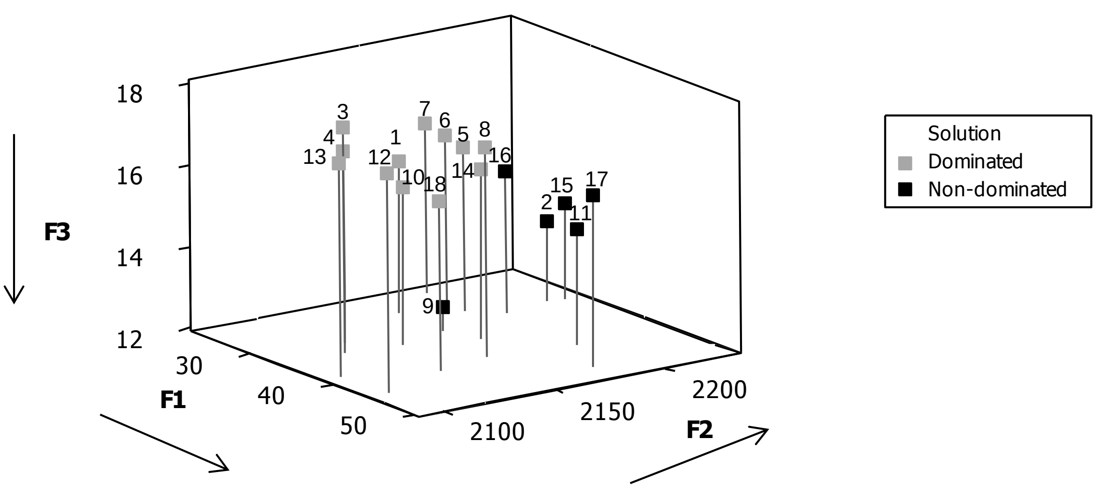

Figure 3.22 Graphical results of the full comparison.

3.5. Discussion of Results

The results obtained from the multiple criteria optimization are the best tradeoff mixtures recommended to the decision makers. Now, the decision makers can select a single mixture among the efficient set presented in this work. They should take the decision based on the characteristics of the mixtures presented in each performance measures. Also, they should consider the proportion of each component in the mixture. This depends on the user's interest about the mineral admixtures.

The efficient mixtures in day 7 were three and they are presented in Table 3.9. In the analysis of day 28, the efficient mixtures were four (Table 3.9). And in the full comparison analysis, there were six mixtures in the Pareto-efficient frontier. However, there are two mixtures that were efficient in all the analysis conducted. These mixtures are: the control mixture with 100% of PC, 0% of FA, and 0% of nS; and the mixture with 78.5% of PC, 20% of FA, and 1.5% of nS. It is interesting that this last one contains the cement replacement by FA and also the silica nanoparticles.

Nevertheless, the mixtures that contained FA but did not contain nS, did not belong to the Pareto-efficient frontier. This behavior was observed in all the analysis. Therefore, the addition of silica nanoparticles appears to be necessary when FA is presented as cement replacement. This is to improve the physical and mechanical properties of the resulting concrete.

Table 3.9 Original average results of the best tradeoffs mixtures in both analysis.

Best Tradeoffs Mixtures	k	Mixture Proportions (PC/FA/nS)	Compressive Strength, Average	Bulk Density, Average	Volume of Permeable Pore Space, Average
			MPa	Kg/m^3	%
7 days	2	1.000/0.00/0.000	31.11	2218.43	13.85
	8	0.785/0.20/0.015	40.40	2156.64	17.00
	9	0.570/0.40/0.030	33.35	2163.49	12.49
28 days	2	1.000/0.00/0.000	41.91	2192.05	14.75
	6	0.985/0.00/0.015	31.29	2226.15	14.25
	7	0.970/0.00/0.030	31.81	2197.49	15.35
	8	0.785/0.20/0.015	47.27	2179.52	16.12
Full Comparison	2	1.000/0.00/0.000	31.11	2218.43	13.85
	9	0.570/0.40/0.030	33.35	2163.49	12.49
	11	1.000/0.00/0.000	41.91	2192.05	14.75
	15	0.985/0.00/0.015	31.29	2226.15	14.25
	16	0.970/0.00/0.030	31.81	2197.49	15.35
	17	0.785/0.20/0.015	47.27	2179.52	16.12

3.6. Final Remarks

Three concrete performance measures were considered in this chapter: concrete compressive strength, bulk density, and percentage of voids (porosity). Nine mixture's proportion combinations were evaluated considering different percentages of PC, FA, and nS. The use of the multiple criteria optimization helped find the mixtures that were the best compromise among the studied objectives. These performance measures were measured after 7 and 28 days. At day 7, three mixtures were part of the Pareto-efficient frontier. Two of them were mixtures with cement replacement, i.e. FA and nS at different levels. On the other hand, four mixtures were part of the Pareto efficient frontier at day

28. This time one mixture has cement replacement (FA and nS). In addition, two mixtures were efficient either in day 7 and day 28.

In this study, a multiple criteria optimization strategy permitted to recommend the use of FA and nS to improve the concrete properties at its early age. However, if the analysis is performed considering only one performance measures, such as compressive strength like in the first stage of this work, the option of cement replacement by FA is not recommended. Hence, taking in consideration several performance measures the use of mineral admixtures is suggested. This is because a mixture with mineral admixtures will be equally efficient than a control mixture with just PC when more properties are considered.

IV. CHAPTER

4. Conclusions and Recommendations

The utilization of design of experiments for mixtures helped characterize concrete properties when mineral admixtures are present keeping in mind that this material has high composition variability (in terms of its individual constituents). In the present work, we first evaluated the mixture components utilizing nonlinear single objective optimization. The percentage gain in compressive strength was obtained by each percentage of nS added in combination with FA.

However, concrete users are interested in different desirable characteristics. Therefore, a multiple criteria approach was followed in order to give a more general recommendation. This is done by evaluating three performance measures, maximizing compressive strength and density and minimizing the material porosity. With the methodology utilized, the results suggested the utilization of conventional concrete mixture but also mixtures containing cement replacement by FA and nS. The methodology helped in the decision making process of mixtures proportions selection. This selection is based on the mixtures mechanical and physical properties evaluated. Now, as the decision makers know the best tradeoffs mixtures, the final recommendation is easier to make.

4.1. Future Work

An important aspect in the construction industry is the inherent costs associated to their projects. As mentioned before, FA is one of the low-priced mineral admixtures. Moreover, the benefits of silica nanoparticles resides on the improvements of the concrete physical and mechanical properties and its low cost of production [14], [64], [65]. Therefore, if different mixtures of PC, FA, and nS are evaluated measuring several performance measures and also considering their associated costs the result will be interested. According Felekoglu [66], the cost of each mixture combinations can be considered as follows:

First calculate the material cost per kilogram.

Table 4.1 Estimated unit cost for each component of the mixture.

Material	PC	FA	nS	Coarse Aggregate	Fine Aggregate	Super-plasticizer	water
Unit cost ($/kg.)	c_1	c_2	c_3	c_4	c_5	c_6	c_7

Then the total mixture cost due to all the materials is computed.

Table 4.2 Total costs associated with each mixture combination.

k	Mixture Proportions (PC/FA/nS)	Total Mixture Cost ($/m^3)
1	0.800/0.20/0.000	h_1
2	1.000/0.00/0.000	h_2
3	0.600/0.40/0.000	h_3
4	0.585/0.40/0.015	h_4
5	0.770/0.20/0.030	h_5
6	0.985/0.00/0.015	h_6
7	0.970/0.00/0.030	h_7
8	0.785/0.20/0.015	h_8
9	0.570/0.40/0.030	h_9

The researchers in the paper mentioned recommend the mixture combination with the lower material cost for unit strength [66]. However, our suggestion for future work is to estimate the costs by the same means but including the total mixture cost as a fourth performance measures, applied the multiple criteria optimization method, and then make a recommendation. Otherwise, if a subjective methodology is followed different results will be obtained because it will depend of the preferences of the researcher. In Appendix 1 a cost analysis was developed based on the local prices of the materials used for the mixtures.

A limitation of the general methodology followed, perhaps, is that the order of the regression model depends of the number of design points selected. In addition, if a greater model adjustment is desired more work and time are required to complete the design of experiments. Therefore, a suggestion for futures investigations in this area is that previously define what they want to specifically know and then execute the experiment to avoid delays during the investigation.

In addition, the concrete density can be evaluated more thoroughly in order to investigate if increasing the concrete compression strength, the total volume required of concrete can be reduced. Also, the use of optical microscopy can be employed to observe and analyze the composition and particles segregation of the different mixtures evaluated.

V. CHAPTER

5. References

[1] J. Thomas and H. Jennings, “Is Concrete an Interesting Material from a Scientific Point of View?,” *Center for Advanced Concrete Based Materials Research*, 2008. .

[2] S. U. Pillai and D. Menon, *Reinforced Concrete Design*. New Delhi: McGraw Hill, 2003.

[3] J. M. Castro, M. C. Ríos, and C. A. Mount-Campbell, “Modelling and simulation in reactive polymer processing,” *Model. Simul. Mater. Sci. Eng.*, vol. 12, no. 3, pp. S121–S149, May 2004.

[4] O. Akalin, K. U. Akay, B. Sennaroglu, and M. Tez, “Optimization of chemical admixture for concrete on mortar performance tests using mixture experiments,” *Chemom. Intell. Lab. Syst.*, vol. 104, no. 2, pp. 233–242, Dec. 2010.

[5] N. M. García, L. E. Zapata, O. M. Suárez, and M. Cabrera-Ríos, “Effect of fly ash and nanosilica on compressive strength of concrete at early age,” *Adv. Appl. Ceram.*, vol. 114, no. 2, pp. 99–106, Feb. 2015.

[6] L. E. Zapata Orduz, A. Caceres, O. Molina, O. M. Suarez, and G. Portela, “RHEOLOGICAL AND MECHANICAL CHARACTERIZATION OF PORTLAND CEMENT MIXES CONTAINING MICRO AND NANO AMORPHOUS SILICA PARTICLES,” University of Puerto Rico-Mayaguez, 2013.

[7] Y.-H. Lin, Y.-Y. Tyan, T.-P. Chang, and C.-Y. Chang, “An assessment of optimal mixture for concrete made with recycled concrete aggregates,” *Cem. Concr. Res.*, vol. 34, no. 8, pp. 1373–1380, Aug. 2004.

[8] R. H. Myers and D. Montgomery, *Response Surface Methodology*. Danvers: John Wiley and Sons, 2002.

[9] K. Hussain, P. Choktaweekarn, and S. Tangtermsirikul, “Effect of Mineral Admixtures on Curing Sensitivity of Concrete,” *Thammasat Int. J. Sc. Tech*, vol. 16, no. 3, pp. 1–8, 2011.

[10] M. Cyr, P. Lawrence, and E. Ringot, “Efficiency of mineral admixtures in mortars: Quantification of the physical and chemical effects of fine admixtures in relation with compressive strength,” *Cem. Concr. Res.*, vol. 36, no. 2, pp. 264–277, Feb. 2006.

[11] J. Sunku, "Advantages of Using Fly Ash as Supplementary Cementing Material (SCM) in Fibre Cement Sheets," *10th Int. Inorganic-Bonded Fiber Compos. Conf.*, pp. 25–32, 2006.

[12] J. Björnström, A. Martinelli, A. Matic, L. Börjesson, and I. Panas, "Accelerating effects of colloidal nano-silica for beneficial calcium–silicate–hydrate formation in cement," *Chem. Phys. Lett.*, vol. 392, no. 1–3, pp. 242–248, Jul. 2004.

[13] A. Bakri, A. M. Mustafa, H. Kamarudin, M. Bnhussain, A. R. Rafiza, and Y. Zarina, "Effect of Na^sub 2^SiO^sub 3^/NaOH Ratios and NaOH Molarities on Compressive Strength of Fly-Ash-Based Geopolymer," *ACI Mater. J.*, no. June, pp. 503–508, 2013.

[14] G. Quercia and H. J. H. Brouwers, "Application of nano-silica (nS) in concrete mixtures," *8th fib PhD Symp. Kgs. Lyngby, Denmark*, 2010.

[15] P. Mondal, S. P. Shah, L. D. Marks, and J. J. Gaitero, "Comparative Study of the Effects of Microsilica and Nanosilica in Concrete," *Transp. Res. Rec. J. Transp. Res. Board*, vol. 2141, no. -1, pp. 6–9, Dec. 2010.

[16] L. Senff, D. Hotza, W. L. Repette, V. M. Ferreira, and J. A. Labrincha, "Effect of nanosilica and microsilica on microstructure and hardened properties of cement pastes and mortars," *Adv. Appl. Ceram.*, vol. 109, no. 2, pp. 104–110, Feb. 2010.

[17] O. Alawode, P. G. Dip, O. I. Idowu, and M. Sc, "Effects of Water-Cement Ratios on the Compressive Strength and Workability of Concrete and Lateritic Concrete Mixes," *Pacific J. Sci. Technol.*, vol. 12, no. 2, pp. 99–105, 2011.

[18] D. Jato-Espino, E. Castillo-Lopez, J. Rodriguez-Hernandez, and J. C. Canteras-Jordana, "A review of application of multi-criteria decision making methods in construction," *Autom. Constr.*, vol. 45, pp. 151–162, Sep. 2014.

[19] R. Ravindrarajah, "Bleeding of fresh concrete containing cement supplementary materials," *9th East Asia-Pacific Conf. …*, no. December, pp. 16–18, 2003.

[20] L. Basheer, J. Kropp, and D. J. Cleland, "Assessment of the durability of concrete from its permeation properties: a review," Mar. 2001.

[21] I. Kaur and R. Siddique, "MECHANICAL PROPERTIES OF HIGH VOLUME FLY ASH (HVFA) CONCRETE SUBJECTED TO ELEVATED TEMPERATURES UP TO MASTER OF ENGINEERING IN," 2005.

[22] Y. Qing, Z. Zenan, K. Deyu, and C. Rongshen, "Influence of nano-SiO2 addition on properties of hardened cement paste as compared with silica fume," *Constr. Build. Mater.*, vol. 21, no. 3, pp. 539–545, Mar. 2007.

[23] W. D. Lindquist, “DEVELOPMENT AND CONSTRUCTION OF LOW-CRACKING HIGH-PERFORMANCE CONCRETE (LC-HPC) BRIDGE DECKS: FREE SHRINKAGE, MIXTURE OPTIMIZATION, AND CONCRETE PRODUCTION,” University of Kansas, 2008.

[24] S. Cho, C. Yang, and R. Huang, “EFFECT OF AGGREGATE VOLUME FRACTION ON THE ELASTIC MODULI AND VOID RATIO OF CEMENT-BASED MATERIALS,” *J. Mar. Sci. Technol.*, vol. 8, no. 1, pp. 1–7, 2000.

[25] E. Ghafari, H. Costa, E. Júlio, A. Portugal, and L. Durães, “The effect of nanosilica addition on flowability, strength and transport properties of ultra high performance concrete,” *Mater. Des.*, vol. 59, pp. 1–9, Jul. 2014.

[26] A. Baykasoğlu, A. Öztaş, and E. Özbay, “Prediction and multi-objective optimization of high-strength concrete parameters via soft computing approaches,” *Expert Syst. Appl.*, vol. 36, no. 3, pp. 6145–6155, Apr. 2009.

[27] K. S. Kulkarni, S. C. Yaragal, and K. S. Babu Narayan, “AN OVERVIEW OF HIGH PERFORMANCE CONCRETE AT ELEVATED TEMPERATURES,” *Int. J. Appl. Eng. Technol.*, vol. 1, no. 1, pp. 48–60, 2011.

[28] M. a Hassanain and R. E. Loov, “Cost optimization of concrete bridge infrastructure,” *Can. J. Civ. Eng.*, vol. 30, no. 5, pp. 841–849, Oct. 2003.

[29] J. Oliver-Sola, A. Josa, J. Rieradevall, and X. Gabarrell, “Enviromental optimization od concrete sidewalks in urban areas,” *Int. J. Life Cycle Assess.*, vol. 14, no. 4, pp. 302–312, 2009.

[30] I. Paya Zaforteza, F. González Vidosa, and V. Yepes Piqueras, “Heuristic optimization of reinforced concrete building frames,” Polytechnic University of Valencia, 2007.

[31] M. Anson-Cartwright, “Optimization of Aggregate Gradation Combinations to Improve Concrete Sustainability,” University of Toronto, 2011.

[32] E. M. R. Fairbairn, M. M. Silvoso, R. D. Toledo Filho, J. L. D. Alves, and N. F. F. Ebecken, “Optimization of mass concrete construction using genetic algorithms,” *Comput. Struct.*, vol. 82, no. 2–3, pp. 281–299, Jan. 2004.

[33] A. Kajetan, J. Olek, V. P. Drnevich, W. J. Weiss, and T. W. West, “Optimization of Mixture Proportions for Concrete Pavements - Influence of Supplementary Cementitious Materials, Paste Content and Aggregate Gradation,” Purdue University, 2009.

[34] B. Şimşek, Y. T. İç, and E. H. Şimşek, "A TOPSIS-based Taguchi optimization to determine optimal mixture proportions of the high strength self-compacting concrete," *Chemom. Intell. Lab. Syst.*, vol. 125, pp. 18–32, Jun. 2013.

[35] A. Rahim, U. K. Sharma, K. Murugesan, a. Sharma, and P. Arora, "Multi-response optimization of post-fire residual compressive strength of high performance concrete," *Constr. Build. Mater.*, vol. 38, pp. 265–273, Jan. 2013.

[36] X. K. Zou, C. M. Chan, G. Li, and Q. Wang, "Multiobjective Optimization for Performance-Based Design of Reinforced Concrete Frames," *J. Struct. Eng.*, vol. 133, no. 10, pp. 1462–1474, 2007.

[37] S. Barakat, K. Bani-Hani, and M. Q. Taha, "Multi-objective reliability-based optimization of prestressed concrete beams," *Struct. Saf.*, vol. 26, no. 3, pp. 311–342, Jul. 2004.

[38] L. A. Sbia, A. Peyvandi, P. Soroushian, A. M. Balachandra, and I. Smith, "Optimization of ultra-high-performance concrete with nano- and micro-scale reinforcement," *Cogent Eng.*, vol. 1, no. 1, p. 990673, Dec. 2014.

[39] C. J. Burgos, J. M. Pizarro, K. I. Camacho-Cáceres, and M. Cabrera-Ríos, "A visual basic tool for Multiple Criteria Optimization," in *Proceedings of the 2014 Industrial and Systems Engineering Research Conference*, 2014, no. i.

[40] B. Rodríguez-Yañez, Y. M. Méndez-Vázquez, and M. Cabrera-Ríos, "Simulation-based Process Windows Simultaneously Considering Two and Three Conflicting Criteria in Injection Molding," *Prod. Manuf. Res.*, 2014.

[41] M. L. Sánchez-Peña, C. E. Isaza, J. Pérez-Morales, C. Rodríguez-Padilla, J. M. Castro, and M. Cabrera-Ríos, "Identification of potential biomarkers from microarray experiments using multiple criteria optimization.," *Cancer Med.*, vol. 2, no. 2, pp. 253–65, Apr. 2013.

[42] E. R. Dunstan, "How Does Pozzolanic Reaction Make Concrete ' Green'?," *2011 World Coal Ash Conf.*, pp. 1–14, 2011.

[43] M. Reiner and K. Rens, "High-Volume Fly Ash Concrete : Analysis and Application," *Pract. Period. Struct. Des. Constr.*, no. February, pp. 58–64, 2006.

[44] D. Montgomery, *Desing and Analysis of Experiment*. Danvers: John Wiley and Sons, 2001.

[45] H. A. Taha, *Operations Research: An Introduction*, 9th ed. New Jersey: Pearson Prentice Hall, 2012.

[46] M. S. Bazaraa, H. D. Sherali, and C. M. Shetty, *Nonlinear Programming Theory and Algorithms*, 3th ed. New York: John Wiley & Sons, 2006.

[47] Microsoft, “Solver Uses Generalized Reduced Gradient Algorithm,” *Article ID: 82890*, 2011. [Online]. Available: http://support.microsoft.com/kb/82890.

[48] L. E. Zapata-Ordúz, G. Portela, and O. M. Suárez, “Weibull statistical analysis of splitting tensile strength of concretes containing class F fly ash, micro/nano-SiO2,” *Ceram. Int.*, vol. 40, no. 5, pp. 7373–7388, Jun. 2014.

[49] M. A. Caldarone, *High-Strenth Concrete: A Practical Guide*, 1st ed. New York: Taylor & Francis, 2009.

[50] C595 / C595M - 14, “Standard Specification for Blended Hydraulic Cements,” *ASTM Int.*, 2014.

[51] C192/C192M − 13a, “Standard Practice for Making and Curing Concrete Test Specimens in the Laboratory,” *ASTM Int.*, pp. 1–8, 2013.

[52] C 470/C 470M – 02a, “Standard Specification for Molds for Forming Concrete Test Cylinders Vertically 1,” *ASTM Int.*, pp. 1–5, 2003.

[53] C39/C39M-12a, “Standard Test Method for Compressive Strength of Cylindrical Concrete Specimens,” *ASTM Int.*, 2012.

[54] D. Montgomery, E. Peck, and G. G. Vining, *Introduction to Linear Regression Analysis*, Fourth Edi. New Jersey: John Wiley and Sons, 2006.

[55] G. Shakhmenko, I. Juhnevica, and A. Korjakins, “Influence of Sol-Gel Nanosilica on Hardening Processes and Physically-Mechanical Properties of Cement Paste,” *Procedia Eng.*, vol. 57, pp. 1013–1021, Jan. 2013.

[56] J. G. Cabrera, P. A. Claisse, and D. N. Hunt, “Measurement of porosity as a predictor of the durability performance of concrete with and without condensed silica fume,” *Adv. Cem. Res.*, vol. 13, no. 4, pp. 165–174, Jan. 2001.

[57] C. Lian, Y. Zhuge, and S. Beecham, “The relationship between porosity and strength for porous concrete,” *Constr. Build. Mater.*, vol. 25, no. 11, pp. 4294–4298, Nov. 2011.

[58] J. Kazjonovs, D. Bajare, and A. Korjakins, “DESIGNING OF HIGH DENSITY CONCRETE BY USING STEEL TREATMENT WASTE,” in *Modern Building Materials, Structures, and Techniques*, 2010.

[59] P. Lawrence, M. Cyr, and E. Ringot, “Mineral admixtures in mortars effect of type, amount and fineness of fine constituents on compressive strength,” *Cem. Concr. Res.*, vol. 35, no. 6, pp. 1092–1105, Jun. 2005.

[60] M. Ehrgott, *Multicriteria Optimization*, Second edi., vol. 39, no. 2. Heidelberg: Springer, 2005.

[61] K. Deb, “Multi-Objective Optimization Using Evolutionary Algorithms : An Introduction,” Kanpur, 2011.

[62] K. I. Camacho, M. Cabrera-Ríos, S. Davila, and J. Seguel, “OPTIMIZATION-DRIVEN META-ANALYSIS: THE SIMULTANEOUS SEARCH FOR CANCER BIOMARKERS WITH MULTIPLE MICROARRAY EXPERIMENTS,” University of Puerto Rico Mayagüez, 2014.

[63] C642-13, “Standard Test Method for Density , Absorption , and Voids in Hardened Concrete 1,” *ASTM Int.*, pp. 1–3, 2013.

[64] H. Yao, Z. You, L. Li, and C. Lee, “Rheological Properties and Chemical Bonding of Asphalt Modified with Nanosilica,” *J. Mater. Civ. Eng.*, no. November, pp. 1619–1630, 2013.

[65] G. Lazzara and S. Milioto, “Dispersions of nanosilica in biocompatible copolymers,” *Polym. Degrad. Stab.*, vol. 95, no. 4, pp. 610–617, Apr. 2010.

[66] B. FELEKOGLU, “Utilisation of Turkish fly ashes in cost effective HVFA concrete production,” *Fuel*, vol. 85, no. 12–13, pp. 1944–1949, Sep. 2006.

6. Appendices

6.1. Appendix 1

Local Cost Estimation for the Mixture Combinations Evaluated

This section includes a local cost analysis for the materials utilized in the mixtures prepared. Table 6.1 present the suppliers of each material used in the mixture. Then, the total cost of each mixture combination was estimated for 1 cubic meter (Table 6.2).

Table 6.1 Suppliers' information about the materials utilized.

Material	Description	Supplier	Supplier Location	Unit Cost
				$/kg.
Portland Cement	Type I	ESSROC San Juan	Dorado, P.R.	**$ 0.17**
Fly Ash	Class F	ESSROC San Juan	Dorado, P.R.	**$ 0.20***
Silica	nanosilica	Nissan Chemical Industries	Texas, U.S.	**$ 10.00**
Coarse Aggregate	gravel	ESSROC San Juan	Dorado, P.R.	**$ 0.02**
Fine Aggregate	processed	ESSROC San Juan	Dorado, P.R.	**$ 0.02**
	beach sand	Boquerón Mini Market and Hardware, Corp.	Rincón, P.R.	**$ 0.03**
Superplastizicer	Polycarboxylate	Darex Puerto Rico	Bayamón, P.R.	**$ 3.37**
water	tap water	Autoridad de Acueductos y Alcantarillados	Mayagüez, P.R.	**$ 0.01**

*The FA is currently imported to Puerto Rico. There is only one supplier that brings it to the island. Consequently, the cost of FA is higher here when compared to the U.S. plants that give this material for free or sell it by a minimum cost.

The estimated cost of the conventional or traditional mixture (100% PC, 0% FA, and 0% nS) was $174.00. This number is higher when compared to the ready mix cost in the local market that is around $120.00 to $130.00. However, this lower cost could be associated with the mass production.

Table 6.2 Total mixture cost associated with each material utilized.

k	Mixture Proportions (PC/FA/nS)	Portland Cement		Fly Ash		Silica		Coarse Aggregate		Fine Aggregate				Super-plastizicer		water		Total Mixture Cost
		Type I		Class F		nanosilica		gravel		processed (40%)		beach sand (60%)		Polycar-boxylate		tap water		
		Unit Cost ($/kg.)																
		$ 0.17		$ 0.20*		$ 10.00		$ 0.02		$ 0.02		$ 0.03		$ 3.37		$ 0.01		
		kg/m^3	$/m^3	kg/m^3	$/m^3	kg/m^3	$/m^3	kg/m^3	$/m^3	kg/m^3	$/m^3	kg/m^3	$/m^3	kg/m^3	$/m^3	kg/m^3	$/m^3	$/m^3
1	0.800/0.20/0.000	537.9	90.8	134.5	26.9	0.0	0.0	1001.4	15.8	172.6	3.0	258.9	8.0	6.7	22.6	199.5	1.1	**168.00**
2	1.000/0.00/0.000	672.4	113.5	0.0	0.0	0.0	0.0	1001.4	15.8	185.0	3.2	277.4	8.5	9.4	31.7	197.8	1.0	**174.00**
3	0.600/0.40/0.000	403.4	68.1	269.0	53.8	0.0	0.0	1001.4	15.8	160.2	2.8	240.3	7.4	4.0	13.6	201.2	1.1	**163.00**
4	0.585/0.40/0.015	383.3	64.7	269.0	53.8	20.2	201.7	1001.4	15.8	156.9	2.7	235.3	7.3	5.2	17.6	187.4	1.0	**365.00**
5	0.770/0.20/0.030	497.6	84.0	134.5	26.9	40.3	403.4	1001.4	15.8	166.0	2.9	249.0	7.7	6.3	21.3	175.6	0.9	**563.00**
6	0.985/0.00/0.015	694.3	117.2	0.0	0.0	21.5	214.7	1066.0	16.8	193.4	3.3	290.1	8.9	9.7	32.7	196.9	1.0	**395.00**
7	0.970/0.00/0.030	632.0	106.7	0.0	0.0	40.3	403.4	1001.4	15.8	178.3	3.1	267.5	8.2	10.1	34.0	175.0	0.9	**572.00**
8	0.785/0.20/0.015	517.7	87.4	134.5	26.9	20.2	201.7	1001.4	15.8	169.3	2.9	253.9	7.8	5.2	17.6	189.3	1.0	**361.00**
9	0.570/0.40/0.030	363.1	61.3	269.0	53.8	40.3	403.4	1001.4	15.8	153.6	2.6	230.4	7.1	5.1	17.0	178.2	0.9	**562.00**

On the other hand, if we evaluate the cost of the other mixture with cement replacement (78.5% PC, 20% FA, and 1.5% nS) that always appeared in the Pareto-efficient, we can see that it have a higher cost ($361.00). This time is important to mention that the FA used in the mixture have a higher cost that the PC and that the cost of the nanoparticles of silica are higher too. This could be due to the small quantities in which we buy them.

In order to make a better cost analysis, the costs of producing these mixtures should be deeply investigated in mass production. Also, the production cost of nanosilica is decreasing due to improvements to the manufacturing process. In addition, the variability of the cost in the market should be considered. However, the performed analysis gives us general information about the current costs in the local market.

6.2. Appendix 2

Regression models from Minitab after removing the insignificant term.

Table 6.3 Estimated Regression Coefficients for Y_1 in pseudocomponents.

Term	Coef	SE Coef	T	P	VIF
PC	20.3	0.3034	*	*	3.11
FA	9.5	0.4746	*	*	6.34
nS	101.9	46.606	*	*	1374.65
PC*FA	-8.1	1.8654	-4.33	0.000	5.5
PC*nS	-71.7	53.6494	-1.34	0.189	596.1
FA*nS	-115.2	54.2279	-2.13	0.040	586.34
PC*FA*nS	64.5	22.057	2.92	0.006	3.97
PC*w/b	-11.7	0.2934	-39.93	0.000	2.91
FA*w/b	-7.4	0.4597	-16.07	0.000	5.94
PC*FA*w/b	8.2	1.8525	4.45	0.000	5.43
PC*nS*w/b	22.5	3.6939	6.09	0.000	2.83
FA*nS*w/b	19.1	4.8009	3.97	0.000	4.6
PC*FA*nS*w/b	-168	21.8029	-7.7	0.000	3.88

Table 6.4 Estimated Regression Coefficients for Y_3 in pseudocomponents.

Term	Coef	SE Coef	T	P	VIF
PC	35.9	0.5486	*	*	3.11
FA	10.8	0.8581	*	*	6.34
nS	167.6	84.2574	*	*	1374.65
PC*FA	2.6	3.3724	0.78	0.440	5.5
PC*nS	-72.4	96.9908	-0.75	0.460	596.1
FA*nS	-61	98.0368	-0.62	0.537	586.34
PC*FA*nS	4.9	39.876	0.12	0.903	3.97
PC*w/b	-16.3	0.5304	-30.73	0.000	2.91
FA*w/b	-7.1	0.831	-8.58	0.000	5.94
PC*FA*w/b	-1.6	3.349	-0.48	0.633	5.43
PC*nS*w/b	1.8	6.678	0.26	0.794	2.83
FA*nS*w/b	-48.8	8.6794	-5.62	0.000	4.6
PC*FA*nS*w/b	-115.1	39.4167	-2.92	0.006	3.88

Table 6.5 Estimated Regression Coefficients for Y_7 in pseudocomponents.

Term	Coef	SE Coef	T	P	VIF
PC	44.56	0.871	*	*	3.11
FA	18.35	1.362	*	*	6.34
nS	69.5	133.783	*	*	1374.65
PC*FA	0.94	5.355	0.18	0.861	5.5
PC*nS	98.95	154.001	0.64	0.524	596.1
FA*nS	96.19	155.662	0.62	0.540	586.34
PC*FA*nS	2.85	63.315	0.05	0.964	3.97
PC*w/b	-18.94	0.842	-22.49	0.000	2.91
FA*w/b	-9.55	1.319	-7.24	0.000	5.94
PC*FA*w/b	-5.96	5.318	-1.12	0.269	5.43
PC*nS*w/b	27.48	10.603	2.59	0.013	2.83
FA*nS*w/b	-79.62	13.781	-5.78	0.000	4.6
PC*FA*nS*w/b	-20.58	62.586	-0.33	0.744	3.88

Table 6.6 Estimated Regression Coefficients for Y_{14} in pseudocomponents.

Term	Coef	SE Coef	T	P	VIF
PC	47.6	0.842	*	*	3.11
FA	25	1.316	*	*	6.34
nS	-164.6	129.262	*	*	1374.65
PC*FA	4.4	5.174	0.86	0.396	5.5
PC*nS	388.2	148.797	2.61	0.013	596.1
FA*nS	337.9	150.402	2.25	0.030	586.34
PC*FA*nS	-8.5	61.175	-0.14	0.890	3.97
PC*w/b	-20.5	0.814	-25.19	0.000	2.91
FA*w/b	-14.8	1.275	-11.6	0.000	5.94
PC*FA*w/b	7.4	5.138	1.44	0.158	5.43
PC*nS*w/b	14.5	10.245	1.41	0.165	2.83
FA*nS*w/b	-54.5	13.315	-4.09	0.000	4.6
PC*FA*nS*w/b	-70.6	60.47	-1.17	0.250	3.88

Table 6.7 Estimated Regression Coefficients for Y_{28} in pseudocomponents.

Term	Coef	SE Coef	T	P	VIF
PC	55.12	0.888	*	*	3.11
FA	32.6	1.389	*	*	6.34
nS	20.95	136.358	*	*	1374.65
PC*FA	13.37	5.458	2.45	0.019	5.5
PC*nS	138.98	156.965	0.89	0.381	596.1
FA*nS	128.14	158.658	0.81	0.424	586.34
PC*FA*nS	-71.63	64.534	-1.11	0.273	3.97
PC*w/b	-22.87	0.858	-26.65	0.000	2.91
FA*w/b	-17.51	1.345	-13.02	0.000	5.94
PC*FA*w/b	1.94	5.42	0.36	0.722	5.43
PC*nS*w/b	23.03	10.807	2.13	0.039	2.83
FA*nS*w/b	-35.27	14.046	-2.51	0.016	4.6
PC*FA*nS*w/b	-96.86	63.79	-1.52	0.137	3.88

6.3. Appendix 3

Detailed results from the multiple-criteria analysis for day 7.

Table 6.8 Comparison among all solutions *n* from objective f_1.

$\boldsymbol{f_1}$**vs.** $\boldsymbol{f_1}$	37.23	33.49	30.89	33.02	34.85	37.56	40.40	24.19	31.25
37.23	0	1000	1000	1000	1000	-1	-1	1000	1000
33.49	-1	0	1000	1000	-1	-1	-1	1000	1000
30.89	-1	-1	0	-1	-1	-1	-1	1000	-1
33.02	-1	-1	1000	0	-1	-1	-1	1000	1000
34.85	-1	1000	1000	1000	0	-1	-1	1000	1000
37.56	1000	1000	1000	1000	1000	0	-1	1000	1000
40.40	1000	1000	1000	1000	1000	1000	0	1000	1000
24.19	-1	-1	-1	-1	-1	-1	-1	0	-1
31.25	-1	-1	1000	-1	-1	-1	-1	1000	0

Table 6.9 Comparison among all solutions *n* from objective f_2.

$\boldsymbol{f_2}$**vs.** $\boldsymbol{f_2}$	2170.43	2117.88	2218.43	2210.75	2149.85	2147.80	2146.33	2179.68	2172.82
2170.43	0	1000	-1	-1	1000	1000	1000	-1	-1
2117.88	-1	0	-1	-1	-1	-1	-1	-1	-1
2218.43	1000	1000	0	1000	1000	1000	1000	1000	1000
2210.75	1000	1000	-1	0	1000	1000	1000	1000	1000
2149.85	-1	1000	-1	-1	0	1000	1000	-1	-1
2147.80	-1	1000	-1	-1	-1	0	1000	-1	-1
2146.33	-1	1000	-1	-1	-1	-1	0	-1	-1
2179.68	1000	1000	-1	-1	1000	1000	1000	0	1000
2172.82	1000	1000	-1	-1	1000	1000	1000	-1	0

Table 6.10 Comparison among all solutions *n* from objective f_3.

$\boldsymbol{f_3}$ **vs.** $\boldsymbol{f_3}$	15.59	13.85	17.42	16.58	15.93	16.00	16.04	17.00	12.49
15.59	0	1000	-1	-1	-1	-1	-1	-1	1000
13.85	-1	0	-1	-1	-1	-1	-1	-1	1000
17.42	1000	1000	0	1000	1000	1000	1000	1000	1000
16.58	1000	1000	-1	0	1000	1000	1000	-1	1000
15.93	1000	1000	-1	-1	0	-1	-1	-1	1000
16.00	1000	1000	-1	-1	1000	0	-1	-1	1000
16.04	1000	1000	-1	-1	1000	1000	0	-1	1000
17.00	1000	1000	-1	1000	1000	1000	1000	0	1000
12.49	-1	-1	-1	-1	-1	-1	-1	-1	0

Table 6.11 Matrix to evaluate the second condition of Pareto.

k	$\boldsymbol{f_1}$ **vs.** $\boldsymbol{f_2}$ **vs.** $\boldsymbol{f_3}$											
1	37.23	2170.43	15.59	1500	3000	0	0	0	0	0	0	0
2	33.49	2117.88	13.85	0	1500	0	0	0	0	0	0	0
3	30.89	2218.43	17.42	0	0	1500	0	0	0	0	3000	0
4	33.02	2210.75	16.58	0	0	0	1500	0	0	0	0	3000
5	34.85	2149.85	15.93	0	3000	0	0	1500	0	0	0	0
6	37.56	2147.80	16.00	0	3000	0	0	0	1500	0	0	0
7	40.40	2146.33	16.04	0	3000	0	0	0	0	1500	0	0
8	24.19	2179.68	17.00	0	0	0	0	0	0	0	1500	0
9	31.25	2172.82	12.49	0	0	0	0	0	0	0	0	1500

6.4. Appendix 4

Detailed results from the multiple-criteria analysis for day 28.

Table 6.12 Comparison among all solutions *n* from objective f_1.

f_1 vs. f_1	44.08	36.65	34.47	39.65	41.97	47.27	46.75	31.29	37.06
44.08	0	1000	1000	1000	1000	-1	-1	1000	1000
36.65	-1	0	1000	-1	-1	-1	-1	1000	-1
34.47	-1	-1	0	-1	-1	-1	-1	1000	-1
39.65	-1	1000	1000	0	-1	-1	-1	1000	1000
41.97	-1	1000	1000	1000	0	-1	-1	1000	1000
47.27	1000	1000	1000	1000	1000	0	1000	1000	1000
46.75	1000	1000	1000	1000	1000	-1	0	1000	1000
31.29	-1	-1	-1	-1	-1	-1	-1	0	-1
37.06	-1	1000	1000	-1	-1	-1	-1	1000	0

Table 6.13 Comparison among all solutions *n* from objective f_2.

f_2 vs. f_2	2181.64	2130.71	2223.88	2226.15	2154.05	2096.61	2125.27	2143.24	2190.80
2181.64	0	1000	-1	-1	1000	1000	1000	1000	-1
2130.71	-1	0	-1	-1	-1	1000	1000	-1	-1
2223.88	1000	1000	0	-1	1000	1000	1000	1000	1000
2226.15	1000	1000	1000	0	1000	1000	1000	1000	1000
2154.05	-1	1000	-1	-1	0	1000	1000	1000	-1
2096.61	-1	-1	-1	-1	-1	0	-1	-1	-1
2125.27	-1	-1	-1	-1	-1	1000	0	-1	-1
2143.24	-1	1000	-1	-1	-1	1000	1000	0	-1
2190.80	1000	1000	-1	-1	1000	1000	1000	1000	0

Table 6.14 Comparison among all solutions *n* from objective f_3.

f_3 vs. f_3	15.77	14.75	17.26	17.17	16.06	14.25	15.35	16.12	16.02
15.77	0	1000	-1	-1	-1	1000	1000	-1	-1
14.75	-1	0	-1	-1	-1	1000	-1	-1	-1
17.26	1000	1000	0	1000	1000	1000	1000	1000	1000
17.17	1000	1000	-1	0	1000	1000	1000	1000	1000
16.06	1000	1000	-1	-1	0	1000	1000	-1	1000
14.25	-1	-1	-1	-1	-1	0	-1	-1	-1
15.35	-1	1000	-1	-1	-1	1000	0	-1	-1
16.12	1000	1000	-1	-1	1000	1000	1000	0	1000
16.02	1000	1000	-1	-1	-1	1000	1000	-1	0

Table 6.15 Matrix for evaluates the second condition of Pareto.

k	f_1 vs. f_2 vs. f_3											
1	44.08	2181.64	15.77	1500	3000	0	0	0	0	0	0	0
2	36.65	2130.71	14.75	0	1500	0	0	0	0	0	0	0
3	34.47	2223.88	17.26	0	0	1500	0	0	0	0	3000	0
4	39.65	2226.15	17.17	0	3000	0	1500	0	0	0	3000	3000
5	41.97	2154.05	16.06	0	3000	0	0	1500	0	0	0	0
6	47.27	2096.61	14.25	0	0	0	0	0	1500	0	0	0
7	46.75	2125.27	15.35	0	0	0	0	0	0	1500	0	0
8	31.29	2143.24	16.12	0	0	0	0	0	0	0	1500	0
9	37.06	2190.80	16.02	0	3000	0	0	0	0	0	0	1500

6.5. Appendix 5

Detailed results from the full comparison analysis between all mixtures.

Table 6.16 Comparison among all solutions n from objective f_1.

f_1 vs. f_1	37.23	33.49	30.89	33.02	34.85	37.56	40.40	24.19	31.25	44.08	36.65	34.47	39.65	41.97	47.27	46.75	31.29	37.06
37.23	0	1000	1000	1000	1000	-1	-1	1000	1000	-1	1000	1000	-1	-1	-1	-1	1000	1000
33.49	-1	0	1000	1000	-1	-1	-1	1000	1000	-1	-1	-1	-1	-1	-1	-1	1000	-1
30.89	-1	-1	0	-1	-1	-1	-1	1000	-1	-1	-1	-1	-1	-1	-1	-1	-1	-1
33.02	-1	-1	1000	0	-1	-1	-1	1000	1000	-1	-1	-1	-1	-1	-1	-1	1000	-1
34.85	-1	1000	1000	1000	0	-1	-1	1000	1000	-1	-1	1000	-1	-1	-1	-1	1000	-1
37.56	1000	1000	1000	1000	1000	0	-1	1000	1000	-1	1000	1000	-1	-1	-1	-1	1000	1000
40.40	1000	1000	1000	1000	1000	1000	0	1000	1000	-1	1000	1000	1000	-1	-1	-1	1000	1000
24.19	-1	-1	-1	-1	-1	-1	-1	0	-1	-1	-1	-1	-1	-1	-1	-1	-1	-1
31.25	-1	-1	1000	-1	-1	-1	-1	1000	0	-1	-1	-1	-1	-1	-1	-1	-1	-1
44.08	1000	1000	1000	1000	1000	1000	1000	1000	1000	0	1000	1000	1000	1000	-1	-1	1000	1000
36.65	-1	1000	1000	1000	1000	-1	-1	1000	1000	-1	0	1000	-1	-1	-1	-1	1000	-1
34.47	-1	1000	1000	1000	-1	-1	-1	1000	1000	-1	-1	0	-1	-1	-1	-1	1000	-1
39.65	1000	1000	1000	1000	1000	1000	-1	1000	1000	-1	1000	1000	0	-1	-1	-1	1000	1000
41.97	1000	1000	1000	1000	1000	1000	1000	1000	1000	-1	1000	1000	1000	0	-1	-1	1000	1000
47.27	1000	1000	1000	1000	1000	1000	1000	1000	1000	1000	1000	1000	1000	1000	0	1000	1000	1000
46.75	1000	1000	1000	1000	1000	1000	1000	1000	1000	1000	1000	1000	1000	1000	-1	0	1000	1000
31.29	-1	-1	1000	-1	-1	-1	-1	1000	1000	-1	-1	-1	-1	-1	-1	-1	0	-1
37.06	-1	1000	1000	1000	1000	-1	-1	1000	1000	-1	1000	1000	-1	-1	-1	-1	1000	0

Table 6.17 Comparison among all solutions n from objective f_2.

f_2 vs. f_2	2170.43	2117.88	2218.43	2210.75	2149.85	2147.80	2146.33	2179.68	2172.82	2181.64	2130.71	2223.88	2226.15	2154.05	2096.61	2125.27	2143.24	2190.80
2170.43	0	1000	-1	-1	1000	1000	1000	-1	-1	-1	1000	-1	-1	1000	1000	1000	1000	-1
2117.88	-1	0	-1	-1	-1	-1	-1	-1	-1	-1	-1	-1	-1	-1	1000	-1	-1	-1
2218.43	1000	1000	0	1000	1000	1000	1000	1000	1000	1000	1000	-1	-1	1000	1000	1000	1000	1000
2210.75	1000	1000	-1	0	1000	1000	1000	1000	1000	1000	1000	-1	-1	1000	1000	1000	1000	1000
2149.85	-1	1000	-1	-1	0	1000	1000	-1	-1	-1	1000	-1	-1	-1	1000	1000	1000	-1
2147.80	-1	1000	-1	-1	-1	0	1000	-1	-1	-1	1000	-1	-1	-1	1000	1000	1000	-1
2146.33	-1	1000	-1	-1	-1	-1	0	-1	-1	-1	1000	-1	-1	-1	1000	1000	1000	-1
2179.68	1000	1000	-1	-1	1000	1000	1000	0	1000	-1	1000	-1	-1	1000	1000	1000	1000	-1
2172.82	1000	1000	-1	-1	1000	1000	1000	-1	0	-1	1000	-1	-1	1000	1000	1000	1000	-1
2181.64	1000	1000	-1	-1	1000	1000	1000	1000	1000	0	1000	-1	-1	1000	1000	1000	1000	-1
2130.71	-1	1000	-1	-1	-1	-1	-1	-1	-1	-1	0	-1	-1	-1	1000	1000	-1	-1
2223.88	1000	1000	1000	1000	1000	1000	1000	1000	1000	1000	1000	0	-1	1000	1000	1000	1000	1000
2226.15	1000	1000	1000	1000	1000	1000	1000	1000	1000	1000	1000	1000	0	1000	1000	1000	1000	1000
2154.05	-1	1000	-1	-1	1000	1000	1000	-1	-1	-1	1000	-1	-1	0	1000	1000	1000	-1
2096.61	-1	-1	-1	-1	-1	-1	-1	-1	-1	-1	-1	-1	-1	-1	0	-1	-1	-1
2125.27	-1	1000	-1	-1	-1	-1	-1	-1	-1	-1	-1	-1	-1	-1	1000	0	-1	-1
2143.24	-1	1000	-1	-1	-1	-1	-1	-1	-1	-1	1000	-1	-1	-1	1000	1000	0	-1
2190.80	1000	1000	-1	-1	1000	1000	1000	1000	1000	1000	1000	-1	-1	1000	1000	1000	1000	0

Table 6.18 Comparison among all solutions n from objective f_3.

f_3**vs.** f_3	15.59	13.85	17.42	16.58	15.93	16.00	16.04	17.00	12.49	15.77	14.75	17.26	17.17	16.06	14.25	15.35	16.12	16.02
15.59	0	1000	-1	-1	-1	-1	-1	-1	1000	-1	1000	-1	-1	-1	1000	1000	-1	-1
13.85	-1	0	-1	-1	-1	-1	-1	-1	1000	-1	-1	-1	-1	-1	-1	-1	-1	-1
17.42	1000	1000	0	1000	1000	1000	1000	1000	1000	1000	1000	1000	1000	1000	1000	1000	1000	1000
16.58	1000	1000	-1	0	1000	1000	1000	-1	1000	1000	1000	-1	-1	1000	1000	1000	1000	1000
15.93	1000	1000	-1	-1	0	-1	-1	-1	1000	1000	1000	-1	-1	-1	1000	1000	-1	-1
16.00	1000	1000	-1	-1	1000	0	-1	-1	1000	1000	1000	-1	-1	-1	1000	1000	-1	-1
16.04	1000	1000	-1	-1	1000	1000	0	-1	1000	1000	1000	-1	-1	-1	1000	1000	-1	1000
17.00	1000	1000	-1	1000	1000	1000	1000	0	1000	1000	1000	-1	-1	1000	1000	1000	1000	1000
12.49	-1	-1	-1	-1	-1	-1	-1	-1	0	-1	-1	-1	-1	-1	-1	-1	-1	-1
15.77	1000	1000	-1	-1	-1	-1	-1	-1	1000	0	1000	-1	-1	-1	1000	1000	-1	-1
14.75	-1	1000	-1	-1	-1	-1	-1	-1	1000	-1	0	-1	-1	-1	1000	-1	-1	-1
17.26	1000	1000	-1	1000	1000	1000	1000	1000	1000	1000	1000	0	1000	1000	1000	1000	1000	1000
17.17	1000	1000	-1	1000	1000	1000	1000	1000	1000	1000	1000	-1	0	1000	1000	1000	1000	1000
16.06	1000	1000	-1	-1	1000	1000	1000	-1	1000	1000	1000	-1	-1	0	1000	1000	-1	1000
14.25	-1	1000	-1	-1	-1	-1	-1	-1	1000	-1	-1	-1	-1	-1	0	-1	-1	-1
15.35	-1	1000	-1	-1	-1	-1	-1	-1	1000	-1	1000	-1	-1	-1	1000	0	-1	-1
16.12	1000	1000	-1	-1	1000	1000	1000	-1	1000	1000	1000	-1	-1	1000	1000	1000	0	1000
16.02	1000	1000	-1	-1	1000	1000	-1	-1	1000	1000	1000	-1	-1	-1	1000	1000	-1	0

Table 6.19 Matrix for evaluates the second condition of Pareto.

k	f_1 vs. f_2 vs. f_3																				
1	37.23	2170.43	15.59	1500	3000	0	0	0	0	0	0	0	0	3000	0	0	0	0	0	0	0
2	33.49	2117.88	13.85	0	1500	0	0	0	0	0	0	0	0	0	0	0	0	0	0	0	0
3	30.89	2218.43	17.42	0	0	1500	0	0	0	0	3000	0	0	0	0	0	0	0	0	0	0
4	33.02	2210.75	16.58	0	0	0	1500	0	0	0	0	3000	0	0	0	0	0	0	0	3000	0
5	34.85	2149.85	15.93	0	3000	0	0	1500	0	0	0	0	0	0	0	0	0	0	0	0	0
6	37.56	2147.80	16.00	0	3000	0	0	0	1500	0	0	0	0	3000	0	0	0	0	0	0	0
7	40.40	2146.33	16.04	0	3000	0	0	0	0	1500	0	0	0	3000	0	0	0	0	0	0	0
8	24.19	2179.68	17.00	0	0	0	0	0	0	0	1500	0	0	0	0	0	0	0	0	0	0
9	31.25	2172.82	12.49	0	0	0	0	0	0	0	0	1500	0	0	0	0	0	0	0	0	0
10	44.08	2181.64	15.77	3000	3000	0	0	0	0	0	0	3000	1500	3000	0	0	0	0	0	0	0
11	36.65	2130.71	14.75	0	3000	0	0	0	0	0	0	0	0	1500	0	0	0	0	0	0	0
12	34.47	2223.88	17.26	0	3000	0	3000	0	0	0	3000	3000	0	0	1500	0	0	0	0	3000	0
13	39.65	2226.15	17.17	3000	3000	0	3000	3000	3000	0	3000	3000	0	3000	0	1500	0	0	0	3000	3000
14	41.97	2154.05	16.06	0	3000	0	0	3000	3000	3000	0	0	0	3000	0	0	1500	0	0	0	0
15	47.27	2096.61	14.25	0	0	0	0	0	0	0	0	0	0	0	0	0	0	1500	0	0	0
16	46.75	2125.27	15.35	0	3000	0	0	0	0	0	0	0	0	0	0	0	0	0	1500	0	0
17	31.29	2143.24	16.12	0	0	0	0	0	0	0	0	0	0	0	0	0	0	0	0	1500	0
18	37.06	2190.80	16.02	0	3000	0	0	3000	0	0	0	3000	0	3000	0	0	0	0	0	0	1500